

CD98hc (*SLC3A2*) regulation of skin homeostasis wanes with age

Etienne Boulter, Soline Estrach, Aurélia Errante, Catherine Pons, Laurence Cailleateau, Floriane Tissot, Guerrino Meneguzzi, and Chloé C. Féral

Institute for Research on Cancer and Aging, Nice (IRCAN), AVENIR Team, University of Nice Sophia-Antipolis, Institut National de la Santé et de la Recherche Médicale U1081, Centre National de la Recherche Scientifique UMR 7284, Centre Antoine Lacassagne, Nice 06107, France

Skin aging is linked to reduced epidermal proliferation and general extracellular matrix atrophy. This involves factors such as the cell adhesion receptors integrins and amino acid transporters. CD98hc (*SLC3A2*), a heterodimeric amino acid transporter, modulates integrin signaling in vitro. We unravel CD98hc functions in vivo in skin. We report that *CD98hc* invalidation has no appreciable effect on cell adhesion, clearly showing that *CD98hc* disruption phenocopies neither *CD98hc* knockdown in cultured keratinocytes nor epidermal $\beta 1$ integrin loss in vivo. Instead, we show that *CD98hc* deletion in murine epidermis results in improper skin homeostasis and epidermal wound healing. These defects resemble aged skin alterations and correlate with reduction of *CD98hc* expression observed in elderly mice. We also demonstrate that *CD98hc* absence in vivo induces defects as early as integrin-dependent Src activation. We decipher the molecular mechanisms involved in vivo by revealing a crucial role of the *CD98hc/integrins/Rho* guanine nucleotide exchange factor (GEF) leukemia-associated RhoGEF (*LARG*)/RhoA pathway in skin homeostasis. Finally, we demonstrate that the deregulation of RhoA activation in the absence of *CD98hc* is also a result of impaired *CD98hc*-dependent amino acid transports.

CORRESPONDENCE

Chloé C. Féral:
chloe.feral@inserm.fr

Abbreviations used: 4OHT, 4-hydroxy-tamoxifen; CFE, colony-forming efficiency; dpp, days post partum; GAP, GTPase activating protein; GEF, guanine nucleotide exchange factor; HF, hair follicle; IFE, interfollicular epidermis; *LARG*, leukemia-associated RhoGEF; RBD, Rho binding domain; ROS, reactive oxygen species.

Homeostasis in adult somatic tissues requires balanced cell proliferation and differentiation. This is strikingly evident in mammalian epidermis, which is primarily composed of keratinocytes lying on a basement membrane made of extracellular matrix components. This stratified epithelium includes major structures such as the interfollicular epidermis (IFE), hair follicles (HFs), and sebaceous glands. In adults, HFs undergo cyclic degeneration (catagen), rest (telogen), and growth (anagen) which define the so-called hair cycle (Alonso and Fuchs, 2006). In addition, hair growth and wound healing both rely on similar processes: keratinocyte proliferation and migration (Ito et al., 2005; Levy et al., 2007; Blanpain and Fuchs, 2009). During homeostasis, IFE is also maintained by actively cycling cells that divide or differentiate (Clayton et al., 2007). Homeostatic imbalance is responsible for the physical changes associated with aging. Such alterations include epidermal proliferation reduction, extracellular matrix composition, and hair loss (Watt and Fujiwara, 2011). Skin aging is associated with disturbed cell adhesion receptors, integrins, and ECM signaling.

E. Boulter and S. Estrach contributed equally to this paper.

Finally, pronounced defects in amino acid contents in the skin are observed with aging potentially involving impaired amino acid transporter activity.

Integrins are heterodimeric transmembrane receptors consisting of an α and a β subunit that link extracellular matrix components to the cytoskeleton. In epidermis, the integrin $\beta 1$ subunit pairs with seven α subunits (Margadant et al., 2010). Confined $\beta 1$ deletion to epidermis using cytochrome-driven promoters results in progressive hair loss and extensive blistering at the dermal-epidermal junction as a result of impaired adhesion of basal keratinocytes to the basement membrane (Brakebusch et al., 2000; Raghavan et al., 2000; Grose et al., 2002). Even though much less severe and delayed, the $\beta 1$ hypomorphic mice ($\beta 1$ *hpm*), expressing reduced level of $\beta 1$ integrins on keratinocytes, develop similar adhesion defect phenotypes as mice with full ablation of the $\beta 1$ integrin gene (*K5- $\beta 1$* mice; Piwko-Czuchra et al., 2009).

© 2013 Boulter et al. This article is distributed under the terms of an Attribution-NonCommercial-Share Alike-No Mirror Sites license for the first six months after the publication date (see <http://www.rupress.org/terms>). After six months it is available under a Creative Commons License (Attribution-NonCommercial-Share Alike 3.0 Unported license, as described at <http://creativecommons.org/licenses/by-nc-sa/3.0/>).

Finally, decrease in epidermal $\beta 1$ integrin expression level is associated with aging, a phenomenon which is accentuated in photo-exposed skin (Bosset et al., 2003; Giangreco et al., 2010).

The transmembrane protein CD98hc participates in amino acid transport and integrin signaling by interacting, in particular, with $\beta 1A$ integrin (Fenczik et al., 1997; Merlin et al., 2001; Rintoul et al., 2002; Feral et al., 2005). CD98 is a heterodimer, in which a unique common heavy chain (4F2hc, CD98hc, SLC3A2) associates with one of several light chains composed of multiple membrane-spanning domains (Devés and Boyd, 2000). Expression of CD98hc in mammalian cells stimulates amino acid transport by promoting cell surface expression of the light chain (Mastroberardino et al., 1998). In addition to its role in amino acid transport, CD98hc interacts with integrins and regulates their signaling properties (Fenczik et al., 1997, 2001; Chandrasekaran et al., 1999; Zent et al., 2000; Kolesnikova et al., 2001; Merlin et al., 2001; Feral et al., 2005). Our studies and those of others have been instrumental in understanding how CD98hc physically and functionally interacts with integrins and regulates their functions in vitro (Merlin et al., 2001; Rintoul et al., 2002; Henderson et al., 2004; Feral et al., 2005, 2007). Knockdown studies in human keratinocytes in vitro concluded the importance of CD98hc for cell adhesion and differentiation by regulating $\beta 1$ integrin trafficking (Lemaître et al., 2011).

Based on these in vitro studies, we hypothesized that conditionally knocking out CD98hc specifically in basal keratinocytes of the epidermis would result in similar adhesion defect phenotypes (i.e., blistering) as was shown for $\beta 1$ integrin mutant mouse models (described above). However, we now demonstrate that in vivo *CD98hc* gene ablation does not lead to a $\beta 1$ integrin-mediated adhesion defect, in contrast to what has been shown in vitro. Instead, we show that, in an age-dependent manner, *CD98hc* deletion in basal keratinocytes induces a major hair cycle delay in young adult mice and impairs skin wound healing as a result of defects in cell proliferation and migration. Its disruption in basal keratinocytes of the epidermis leads, in vivo, to aberrant integrin-downstream signaling such as Src inhibition and persistent RhoA activation. We show that persistent RhoA activation is a result of both activation of the RhoA-specific guanine nucleotide exchange factor (GEF) AHRGEF12/leukemia-associated RhoGEF (LARG) and accumulation of reactive oxygen species (ROS), as a consequence of an amino acid transport defect. Our findings demonstrate that, because of its crucial in vivo role in cell proliferation and migration, CD98hc provides keratinocytes with a selective advantage when these cells need to be efficiently and massively recruited, in particular with high epidermal renewal (hair growth and wound healing). Consistently, its expression is reduced in aged epidermis. In conclusion, we show that the in vivo role of CD98hc in keratinocytes is not in cell adhesion but, instead, in cell proliferation and migration through modulating integrin signaling by the Src-RhoA pathway.

RESULTS

CD98hc expression is ablated in the epidermis and HFs of mice after 4-hydroxy-tamoxifen (4OHT) treatments

CD98hc is expressed in human and mouse skin epidermal keratinocytes (Fig. 1, A and H). Primarily found in the basal layer of the epidermis, its expression drastically decreases in the supra-basal layers where keratinocytes undergo differentiation. High expression is also detected at the base of the HF in a region crucial for hair cycle and defined as the bulb (Fig. 1 H). To examine the function of CD98hc in epidermal homeostasis and to circumvent the embryonic lethality of conventional gene-targeted mice for CD98hc (Tsumura et al., 2003), mice carrying loxP-flanked CD98hc alleles (*CD98hc^{fl/fl}*), previously generated (Féral et al., 2007), were crossed with transgenic mice carrying a tamoxifen-inducible Cre-recombinase under the control of the cytokeratin 14 promoter (*K14CreER^{T2}*; Hong et al., 2004; Fig. 1 B). Every other day, a 4OHT or vehicle topical treatment was performed on the back of each mouse (six applications total). Tissue samples were collected 2 wk later (Fig. 1 C). Efficiency and specificity of CD98hc floxed deletion was assessed by both PCR on genomic DNA and immunofluorescence on isolated treated skin samples. As expected, the CD98hc floxed allele was recombined specifically in the epidermis and not in the dermis of 4OHT-treated animals (Fig. 1 D). Accordingly, CD98hc protein was not detectable in the epidermis of 4OHT-treated mice (IFE and HFs), although it was expressed at normal levels in control mice (Fig. 1 H).

K14CreER^{T2}-mediated deletion of CD98hc in young adult mice results in loss of epidermal homeostasis and impaired HF growth, which last for 1 yr

We investigated the effect of epidermal CD98hc deletion in young adult mice in vivo. To do so, 4OHT was applied to the dorsal skin of 19-d-old mice for six treatments (Fig. 1 C). Such an early start treatment was chosen to ensure completion of 4OHT application before the first synchronous hair growth of adult life (Alonso and Fuchs, 2006) and, thus, to achieve an optimal CD98hc deletion in the epidermis. As described earlier, CD98hc protein deficiency was confirmed in vivo. Strikingly, even though CD98hc interacts with $\beta 1$ integrins (Brakebusch et al., 2000; Raghavan et al., 2000) and was recently shown to regulate human keratinocyte adhesion in vitro (Lemaître et al., 2011), its loss in epidermis did not phenocopy the skin blistering, a consequence of a defect in cell adhesion, induced by $\beta 1$ integrin epidermal deletion.

At the start of the first synchronous anagen phase, 4OHT-treated *K14-CreER^{T2}; CD98hc^{fl/fl}* mice presented a drastic delay in HF growth (Fig. 1, B and E), which exceeded a 4-wk period (Fig. 1, F and G). To investigate the HF cycle defect in CD98hc-deficient mice, hematoxylin and eosin (H&E) staining of back skin was performed at different time points (Fig. 1 E, 30 d post partum [dpp30]; Fig. 1 F, dpp51; and Fig. 1 G, dpp65). Although vehicle-treated skin appeared to be in full anagen at dpp30, 4OHT-treated skin had not yet initiated the anagen phase. At dpp51, the phenotype was dramatically aggravated, and only aberrant HF growth occurred in mutant mice. Finally,

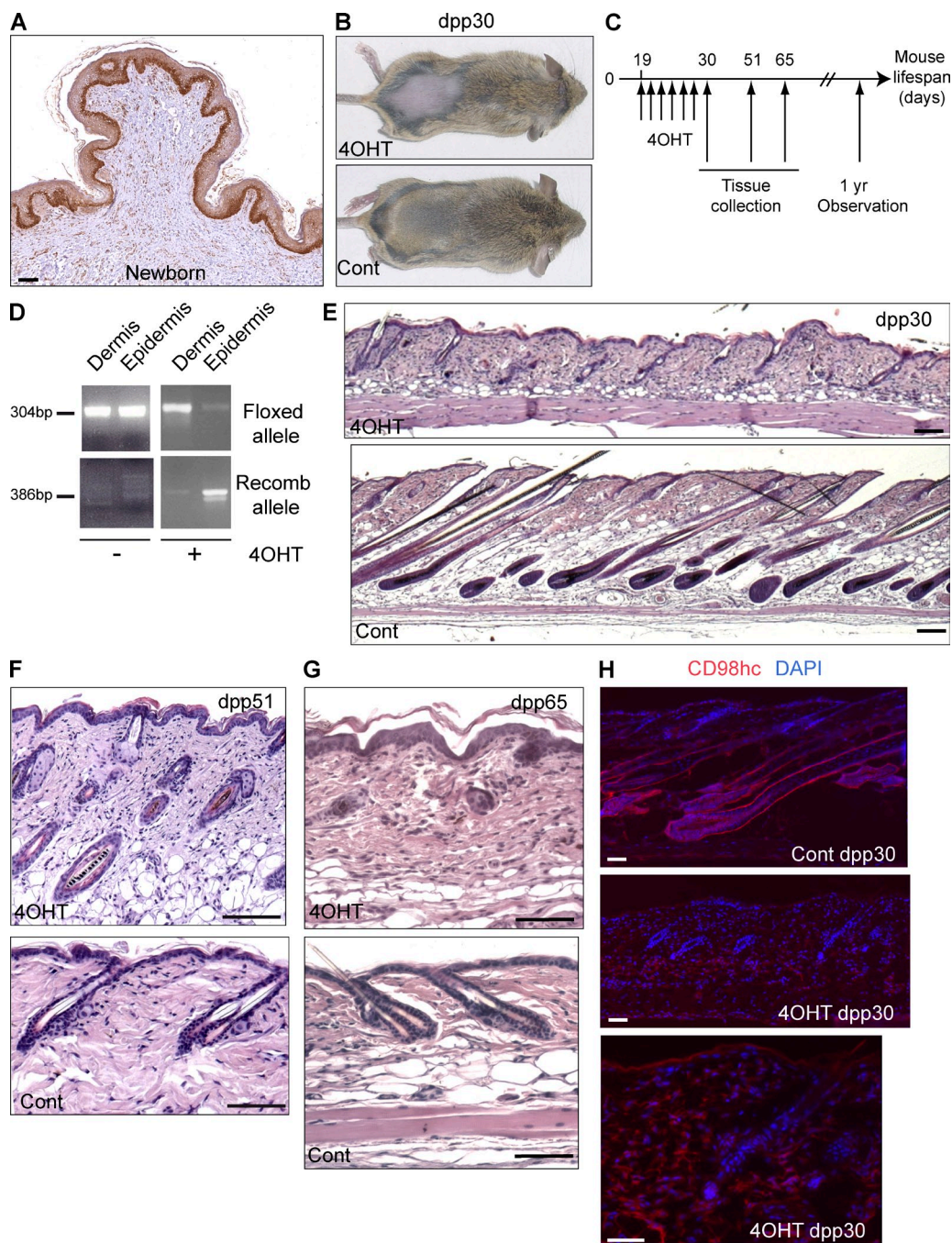


Figure 1. CD98hc deficiency in the epidermis of young adult mice results in major hair growth delay. (A) Immunohistochemical analysis of human foreskin with antibody against CD98hc, showing a strong expression in the basal keratinocyte layer (bar, 125 μ m). (B) K14-CreER²; CD98hc^{fl/fl} mice, treated with vehicle or 4OHT, at dpp30. (C) Young adult mice treatment protocol. (D) Genomic DNA PCR reaction on dermis and epidermis isolated from 4OHT- and vehicle-treated K14-CreER²; CD98hc^{fl/fl} mice. (E–G) Histological images of back skin sagittal sections from a mouse at dpp30 (E; $n = 15$ per group), dpp51 (F; $n = 4$ per group), and dpp65 (G; $n = 6$ per group) with epidermal deletion of the *CD98hc* gene (4OHT) versus an age-matched control (Cont; bars: [E] 125 μ m; [F and G] 50 μ m). (H) Immunofluorescence analysis of mouse skin with epidermal deletion of the *CD98hc* gene (4OHT) versus control (Cont) at dpp30 with antibody against CD98hc (bars, 50 μ m).

at dpp65, control skin reached resting phase, whereas 4OHT-treated skin displayed many aberrant HF. Comparison of HF numbers per surface area at dpp30 versus dpp65, in 4OHT- and vehicle-treated mice, indicated that CD98hc deletion results in a

delay in anagen induction rather than HF loss (Fig. 1 E). Hair growth delay was confirmed by evaluating the expression levels of well described full anagen markers (Estrach et al., 2006), using qPCR, on 4OHT- and vehicle-treated skin samples

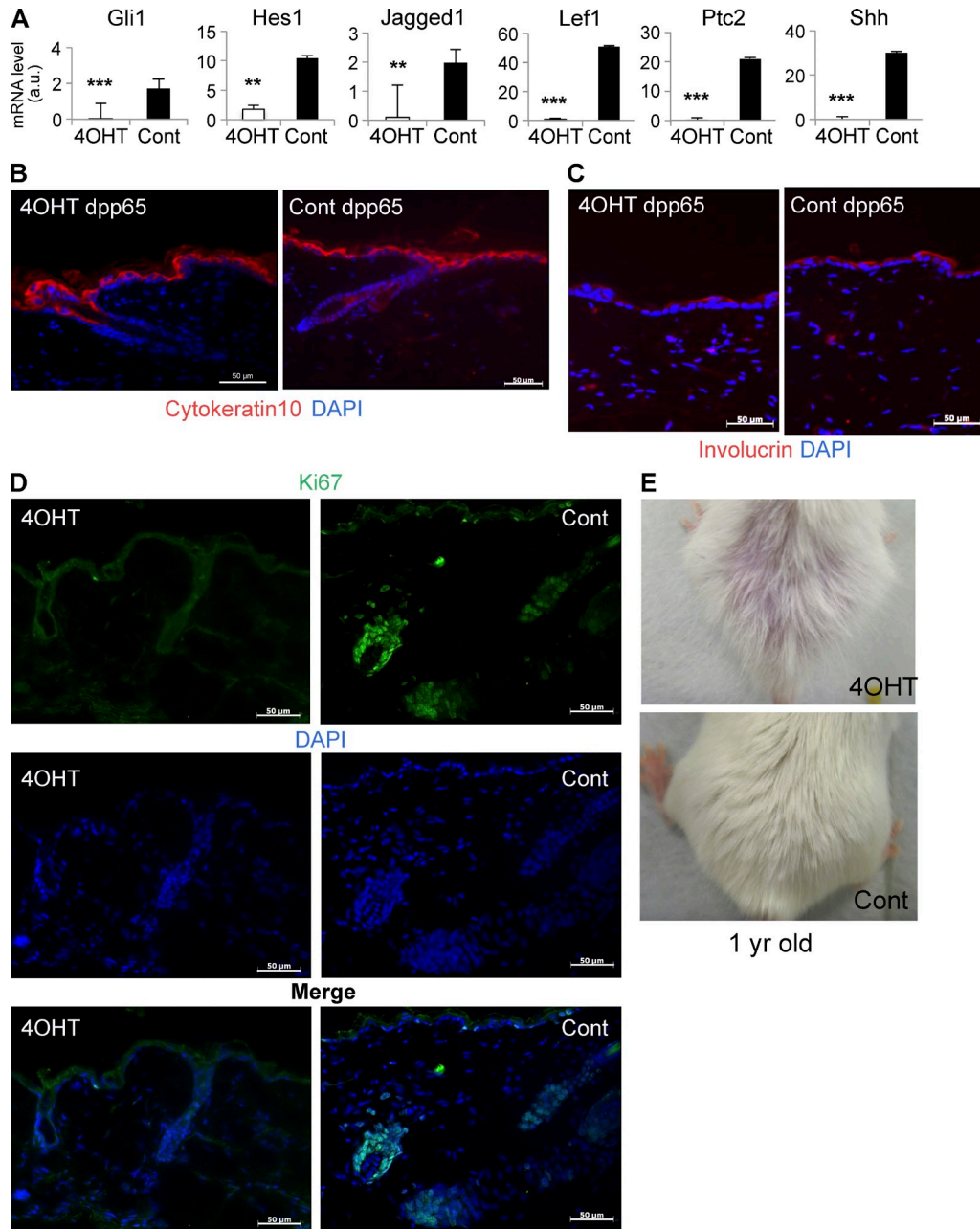


Figure 2. Hair growth defect in CD98hc-deficient epidermis extends beyond 1 yr with major proliferation impairment. (A) Quantitative RT-PCR of full-hair growth markers from K14-CreER^{T2}; CD98hc^{fl/fl} mice with epidermal deletion of the *CD98hc* gene (4OHT) versus control (Cont, treated with vehicle), at dpp30. $n = 5$ per group. Data are shown as mean \pm SEM. **, $P < 0.01$; ***, $P < 0.001$. GAPDH mRNA level was used as a housekeeping gene (not depicted). (B and C) Immunofluorescence analysis of mice skin with epidermal deletion of the *CD98hc* gene (4OHT) versus control (Cont) at dpp65 with antibody against cytokeratin 10 (B) or involucrin (C). Bars, 50 μ m. (D) Immunofluorescence analysis of mice skin with epidermal deletion of the *CD98hc* gene (4OHT) versus control (Cont) at dpp30 with antibody against proliferation marker Ki67. Visualization of nuclei by DAPI staining. Bars, 50 μ m. (E) Long-term consequence of early CD98hc deletion in epidermis. Treated area with 4OHT or vehicle (cont) from 1-yr-old K14-CreER^{T2}; CD98hc^{fl/fl} mice.

(dpp30; Fig. 2 A). The expression pattern of keratinocyte differentiation markers cytokeratin 10 (K10) and involucrin (Fig. 2, B and C) was normal in CD98hc-null epidermis.

HF cycle relies on a fine balance between proliferation and apoptosis of HF keratinocytes. Thus, we further analyzed the defect in HF growth and in anagen entry in 4OHT-treated

K14-CreER^{T2}; CD98hc^{fl/fl} by Ki67 staining (Fig. 2 D), which revealed major in vivo cell proliferation impairment in CD98hc-deficient epidermis compared with controls. In addition, as determined by TUNEL assay in skin sections, no increase in the apoptosis of HF keratinocytes was observed in CD98hc-deficient epidermis (unpublished data). Finally, HFs

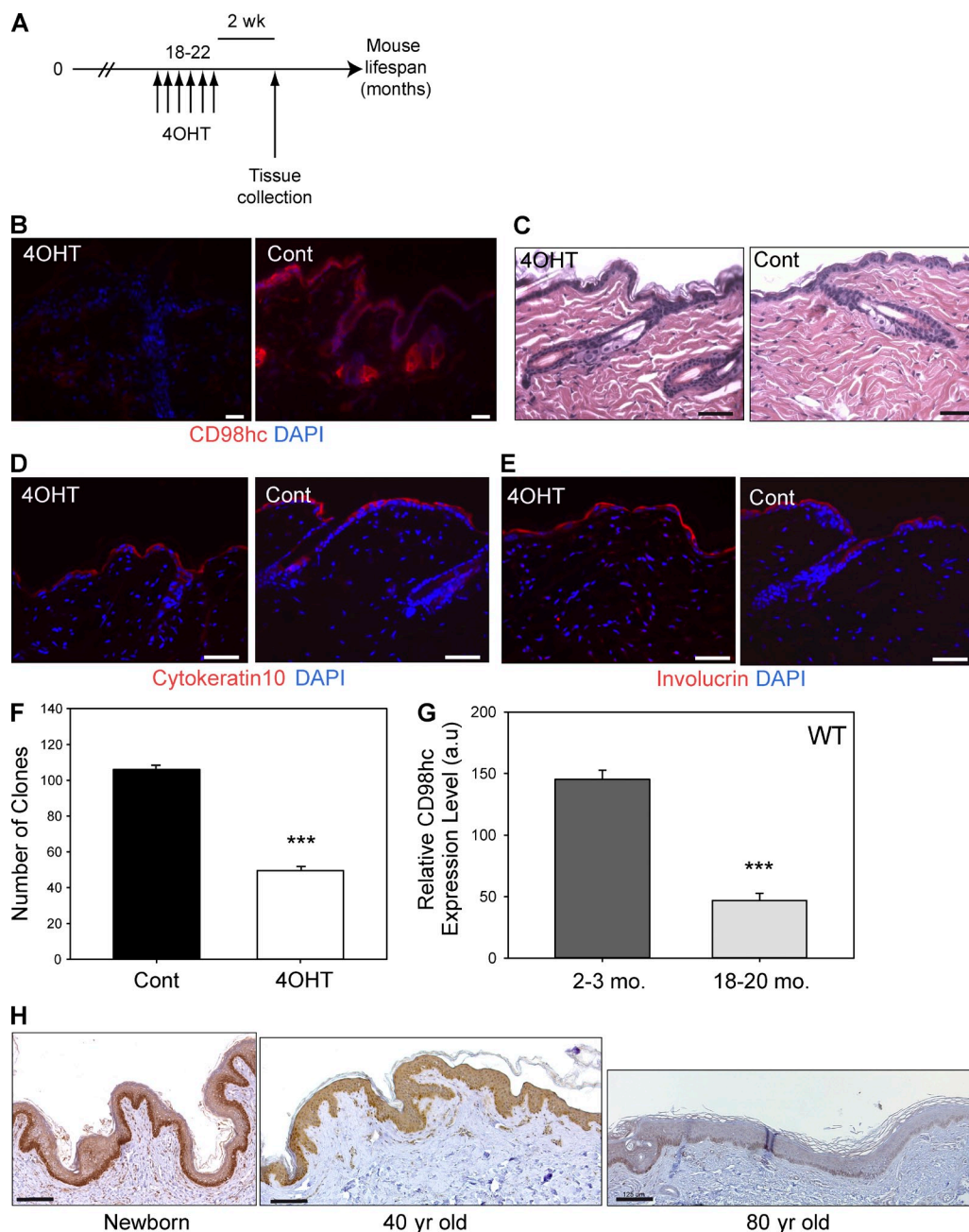


Figure 3. CD98hc deficiency in the epidermis of elderly mice presents a restricted defect in self-renewal ability in vitro. (A) Elderly mice treatment protocol. (B) CD98hc staining analysis on back skin sections from mice at 18–22 mo of age treated with either 4OHT or vehicle (Cont). Bars, 50 μ m. (C) Histological images of back skin sagittal sections from mice at 18–22 mo of age treated with either 4OHT or vehicle (Cont). (D and E) Immunofluorescence analysis of mice skin with epidermal deletion of the *CD98hc* gene (4OHT) versus controls (Cont) with antibody against cytokeratin 10 (D) or involucrin (E). $n = 4$ per group (bars, 50 μ m). (F) CFE evaluation, by quantification of clone numbers, using primary keratinocytes from the dorsal epidermis of vehicle- (Cont) and 4OHT- treated elderly K14-CreER^{T2}; *CD98hc*^{fl/fl} mice (mean \pm SEM, $n = 6$ per group). ***, $P < 0.001$. (G) Relative membrane expression level of CD98hc protein measured by FACS on primary keratinocytes isolated from WT young (2–3 mo old) and elderly (18–20 mo old) mice (mean \pm SEM, $n = 5$ per group). ***, $P < 0.001$. (H) Immunohistochemical analysis of human epithelial samples at different times, newborn ($n = 4$), 40 yr old ($n = 2$), and 80 yr old ($n = 7$) with antibody against CD98hc (bars, 125 μ m).

only partially recovered and supported hair growth 1 yr after CD98hc deletion in the epidermis (Fig. 2 E). Thus, HF cycle defects strongly suggest a major role for CD98hc in preserving the proliferative function of basal keratinocytes localized in the bulb.

CD98hc loss in epidermis of elderly mice induces a restricted effect on in vitro self-renewal ability

During aging, epidermal renewal decreases (Levy et al., 2007). Because CD98hc plays a major role in epidermal homeostasis

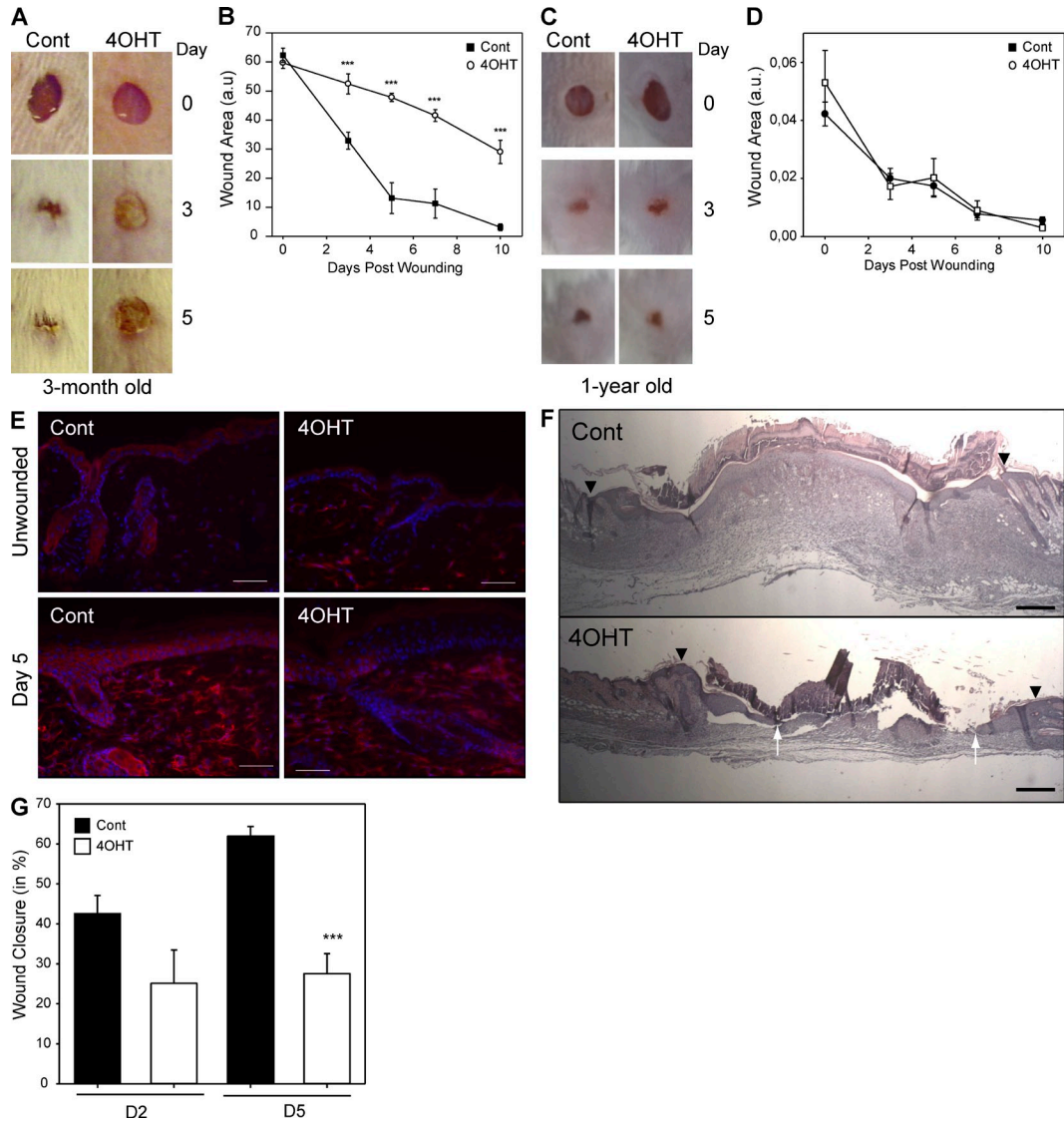


Figure 4. CD98hc deletion impairs wound healing in vivo. (A) Wound closure from 5-mm punch on vehicle- (Cont) or 4OHT-treated skin of K14-CreER^{T2}; CD98hc^{fl/fl} mice over 5 d. (B) Graph representing the wound area measured at different time points after wounding (days 0, 3, 5, 7, and 10) from back skin of vehicle (Cont) or 4OHT-treated K14-CreER^{T2}; CD98hc^{fl/fl} mice ($n = 3$ minimum per group and per genotype). (C) Long-term effect of CD98hc deficiency in the epidermis during wound closure, as described above, of 1-yr-old K14-CreER^{T2}; CD98hc^{fl/fl} mice over 5 d ($n = 5$ for vehicle and $n = 4$ for 4OHT). (D) Graph representing the wound area measured at different time points after wounding (days 0, 3, 5, 7, and 10) from 1-yr-old back skin of vehicle (Cont) or 4OHT-treated K14-CreER^{T2}; CD98hc^{fl/fl} mice to quantify long term effect of CD98hc deficiency in the epidermis during wound closure. (E) Immunofluorescence analysis of CD98hc expression on unwounded and wounded (day 5) sections from long-term-treated mice. Bars 50 μ m. (F) H&E-stained sections depicting wound closure at 7 d after wounding in vehicle- (Cont) or 4OHT (4OHT)-treated skin from K14-CreER^{T2}; CD98hc^{fl/fl} mice. Arrowheads indicate the border of the wound, and white arrows point to the edges of migrating epidermal tongues (note that WT epidermis is already fully closed). Bars, 200 μ m. (G) Measurement of healing rate (wound closure) at days 2 and 5 after wounding, from histological images of 4OHT- (open bars) versus vehicle (black bars)-treated skin of K14-CreER^{T2}; CD98hc^{fl/fl} mice. Depicted are the means \pm SEM of six wounds per time point pooled from two experiments. ***, $P < 0.001$.

of young adult mice, we sought to investigate the effect of CD98hc epidermal deletion in elderly mice. To do so, 18–22-mo-old mice were treated with either 4OHT or vehicle. 2 wk after the last treatment, skin was isolated (Fig. 3 A). Efficient and specific CD98hc deletion in basal keratinocytes of 4OHT-treated skin was confirmed by immunofluorescence staining (Fig. 3 B). Similarly to young mice, no β 1 integrin-related adhesion defect was observed in vivo in CD98hc-null epidermis compared with WT (Fig. 3 C). Elderly CD98hc-null

epidermis mice displayed no visible aberrant phenotype and were grossly indistinguishable from WT controls (Fig. 3, B and C). Immunofluorescent staining of K10 and involucrin on skin sections revealed normal expression pattern in 4OHT-treated mice (Fig. 3, D and E, respectively). Although collectively these results seem to indicate that CD98hc is dispensable for normal epidermal homeostasis in elderly mice, in vitro clone formation efficiency of elderly 4OHT-treated keratinocytes was 2.5 \times less than vehicle-treated ones (Fig. 3 F).

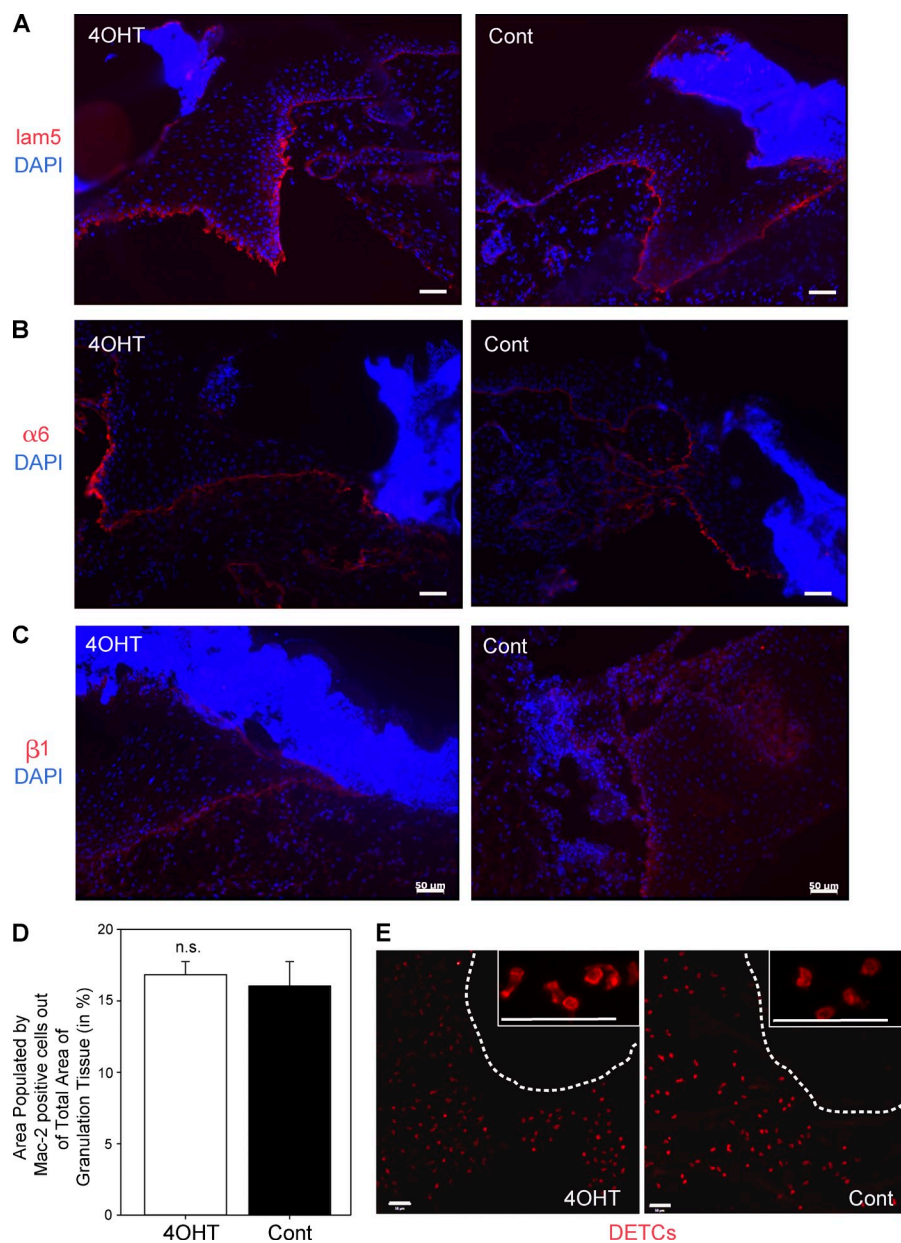


Figure 5. CD98hc deletion does not affect the inflammation response, matrix deposition, or integrin expression during wound healing. (A, B, and C) Immunofluorescence analysis of back wound sections at day 5 with specific antibodies for basal membrane protein (laminin 332, lam5; A), $\alpha 6$ ($\alpha 6$; B), and $\beta 1$ integrins (C). Bars, 50 μm . (D) Quantification of the area covered by MAC2-positive cells in the granulation tissue. Depicted are the means \pm SEM (n.s., not significant). (E) Immunofluorescence analysis of dendritic epidermal T cells (DETCs) on epidermal sheets isolated from ear punches from K14-CreER^{T2}; CD98hc^{fl/fl} mice (4OHT- or vehicle-treated). Insets represent magnified images of the stained area. Bars, 50 μm .

Importantly, we observed a threefold reduction in CD98hc expression levels in WT basal keratinocytes in elderly (18–20 mo old) mice compared with young (2–3 mo old) mice (Fig. 3 G), which correlated with a 1.5-fold decrease of *in vitro* self-renewal ability of WT keratinocytes (comparison of Cont in Fig. 3 F vs. Fig. 7 B). Importantly, we found that CD98hc expression in human skin also decreases with aging specifically in keratinocytes (Fig. 3 H). These data seem to indicate that CD98hc participates in self-renewal capacity in a dose-dependent manner.

CD98hc is required for rapid and efficient repopulation of wounded epidermis

In response to wounding, basal keratinocytes from the wound edge migrate and proliferate to rapidly repopulate the bed of the wounded epidermis (Schäfer and Werner, 2007). To test

the role of CD98hc during wound closure, the backs of young mice (in resting phase, 8 wk old) were treated for 10 d with either vehicle or 4OHT, and then 5-mm punch biopsies were generated at the end of the treatment (Fig. 4, A and B). To avoid any effect of hair growth on healing, skins were in resting phase (telogen) at the time of wounding. In control mice, efficient closure of open wound area was observed in the early phase of healing (sixfold from days 0 to 5). In contrast, it was limited to 1.3-fold in CD98hc-deficient epidermis. Incomplete wound closure was observed in CD98hc-null mice as late as day 10, whereas full healing was achieved in controls. These data were consistent with wound closure kinetics assessed by measuring the distance between the wound edges, which revealed that, at day 5, wound closure in CD98hc-null epidermis was twofold less efficient compared

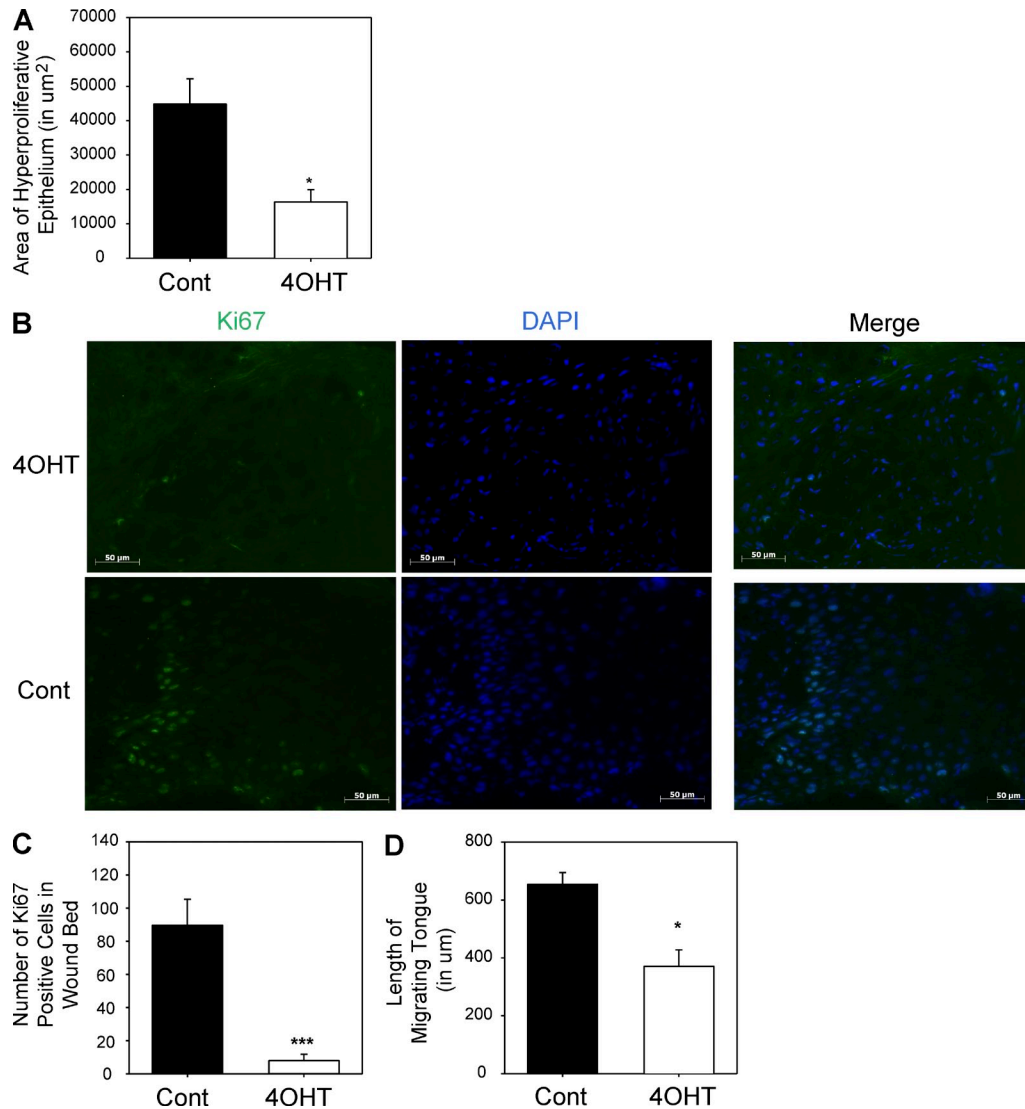


Figure 6. CD98hc is required for rapid and efficient epidermal proliferation and migration in vivo. (A) Determination of proliferation state of the reepithelializing wounds by area measurement of hyperproliferative epithelium of 4OHT- (white bars) versus vehicle (black bars)-treated skin of K14-CreER^{T2}; CD98hc^{fl/fl} mice at day 5 after wounding. $n = 6$ per group. Depicted are the means \pm SEM. *, $P < 0.05$. (B) Immunofluorescence analysis with Ki67 antibody of mice skin treated with either vehicle (Cont) or 4OHT, 5 d after wounding. Cells were costained with DAPI to indicate total number of cells present. Bars, 50 μm . (C) Quantification of Ki67-positive cells in wound bed, determined by counting total number of Ki67-positive cells per field ($n = 6$ per group, means \pm SEM). ***, $P < 0.001$. (D) Evaluation of epidermal migration by measuring the length covered by the migrating tongues of vehicle- (black bars) versus 4OHT (open bars)-treated skin of K14-CreER^{T2}; CD98hc^{fl/fl} mice at day 5 after wounding ($n = 6$ per group, means \pm SEM). *, $P < 0.05$.

with controls (Fig. 4, F and G). Long-term consequences of CD98hc deletion on wound healing were determined by performing similar punch experiments 1 yr after the 4OHT or vehicle treatment on back skin (Fig. 4, C and D). Notably, it seems that long-term CD98hc deletion has only a limited effect on wound repair, as 4OHT-treated mice healed as efficiently as vehicle-treated ones. By performing CD98hc immunofluorescent analysis on the back skin of these mice (1 yr after the 4OHT or vehicle treatment), we noticed the presence, in patches, of CD98hc-expressing keratinocytes in 4OHT-treated skin, in particular during wounding healing (Fig. 4 E). The contribution of these cells could explain the

limited long-term effects observed in these 4OHT-treated mice, during both wound repair (Fig. 4, C and D) and HF regrowth (Fig. 2 E).

In addition to basal keratinocyte proliferation and migration at the wound site, optimal epidermal healing relies on appropriate inflammation and proper synthesis, cross-linking, and alignment of extracellular matrix proteins to provide strength to the healing tissue (Gosain and DiPietro, 2004; Mathieu et al., 2006). Besides, given CD98hc role in regulating integrins, we also performed immunostaining for integrins. Notably, no difference in deposition of the matrix protein laminin332 (Fig. 5 A, lam5), in integrin expression

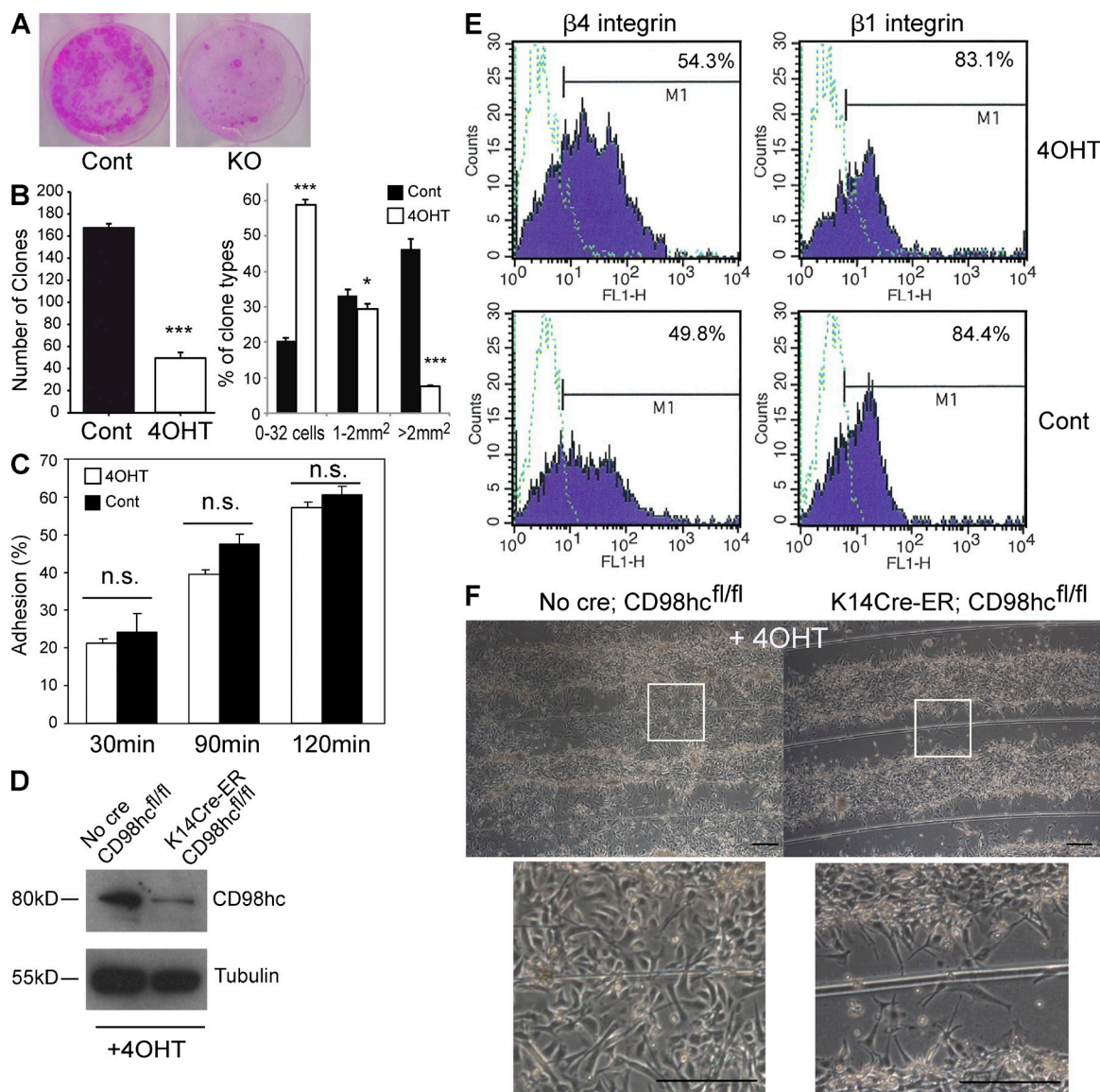


Figure 7. CD98hc is required for efficient keratinocyte proliferation and migration in vitro. (A) Primary keratinocytes from the dorsal epidermis of vehicle- (Cont) and 40HT (KO)-treated K14-CreER^{T2}; CD98hc^{fl/fl} mice were isolated and plated at clonal density. Dishes were stained with rhodamine blue after 2 wk of culture. (B) Evaluation of CFE by quantification of clone numbers \pm SEM, $n = 10$ per group. ***, $P < 0.001$ (left). Analysis of clone types according to the size of the colonies is also represented as percentage of total clones. Depicted are the means \pm SEM (n.s., not significant). *, $P < 0.05$; ***, $P < 0.001$ (right). (C) Adhesion capacity of freshly isolated primary basal keratinocytes on type I collagen at different time points. (D) CD98hc and tubulin expression levels, evaluated by Western blot, from cells used in migration assay. (E) $\beta 1$ and $\beta 4$ integrin expression level by flow cytometric analysis on primary keratinocytes isolated from the dorsal epidermis of vehicle- (Cont) and 40HT (KO)-treated K14-CreER^{T2}; CD98hc^{fl/fl} mice. (F) In vitro migration of 40HT-treated keratinocytes isolated from no cre; CD98hc^{fl/fl} and K14-CreER^{T2}; CD98hc^{fl/fl} mice 24 h after scratching. Insets are magnified images of each field (bars, 100 μ m).

and epitope localization (Fig. 5, B [$\alpha 6$] and C [$\beta 1$]), or in inflammation response (Fig. 5, D and E) was observed in CD98hc-deficient epidermis with respect to control epidermis, excluding a CD98hc-induced defect in matrix remodeling or inflammation during epidermal repair. Altogether, these results disclose that epidermis relies on CD98hc expression for efficient and rapid healing in vivo and suggest that it could be via the role of CD98hc in both cell proliferation and migration.

Keratinocyte proliferation and migration during reepithelialization is CD98hc dependent

Wound reepithelialization is a crucial step in healing process in which the injured area is lined with a protective neo epithelium (Martin, 1997; Singer and Clark, 1999). Keratinocyte proliferation and migration are early events in reepithelialization. Histological examination revealed that CD98hc-null keratinocytes are impaired in their capacity to reepithelialize (Fig. 4, F and G), which, according to measurement of

hyperproliferative epithelium areas (Fig. 6 A), is consistent with a major defect in cell proliferation. Proliferation deficiency was confirmed *in vivo* by quantifying Ki67-positive cells on day 5 wounds (Fig. 6, B and C). Primary keratinocytes were also isolated from the back skin of both 4OHT-treated K14-CreER^{T2}; CD98hc^{fl/fl} and CD98hc^{fl/fl} mice, and identical numbers of cells were plated at clonal density on a feeder layer. Cells were grown for 2 wk and then fixed, stained, and quantified to determine their colony-forming efficiency (CFE; Fig. 7 A). CD98hc-deficient cells formed four times fewer clones than WT cells (Fig. 7 B, left); furthermore, a majority of them was abortive (Fig. 7 B, right). Abortive clones correspond to cells that had divided a maximum of approximately five times (i.e., fewer than 32 cells per colony), and by 14 d almost all of the cells had initiated terminal differentiation (Jones and Watt, 1993). Moreover, we quantified the relative number of clones presenting a low level of proliferation (1–2 mm²) and clones with high level of proliferation (>2 mm²; Jones and Watt, 1993; Fig. 7 B, right). We showed unequivocally that deletion of CD98hc decreases the proportion of highly proliferative clones in favor of abortive clones. These results further strengthened the notion that CD98hc is crucial during keratinocyte proliferation *in vitro* and suggest that its absence influences keratinocyte differentiation. Consistent with the *in vivo* phenotype, no adhesion defect was observed in CD98hc-null primary keratinocytes compared with controls, when plated on type I collagen (Fig. 7 C). CD98hc deletion was confirmed by Western blot analysis (Fig. 7 D). Given CD98hc's role in modulating integrin function, integrin expression profiles were determined and no detectable modification could be observed in CD98hc-null versus control keratinocytes (Fig. 7 E).

Reepithelialization also relies on epidermal cell migration, which can be quantified *in vivo* by measuring the length of the epithelial tongues migrating from the edges of the wound. In CD98hc-null epidermis, measurements highlighted an *in vivo* migration defect, evaluated as a 1.7-fold inhibition compared with control epidermis (Fig. 6 D). Control and CD98hc-KO primary keratinocyte monolayers were also injured *in vitro* using a mechanical scratching device previously used to recapitulate aspects of skin wound reepithelialization (Turchi et al., 2002). Control keratinocytes started to migrate into the scratched cell-free surface of the dish as early as 4 h, which was totally filled 24 h later (Fig. 7 F). In contrast, CD98hc-null primary keratinocytes displayed a drastically reduced migration, at all time points tested, up to 24 h (Fig. 7 F). Thus, altogether these results demonstrate that wound reepithelialization delay *in vivo* in mice deficient for CD98hc in basal keratinocytes is a result of decreased proliferation and migration.

CD98hc-deficient epidermis displays a strong *in vivo* c-Src activation defect

CD98hc deletion *in vitro* impairs integrin-dependent functions, in particular as a result of a FAK phosphorylation defect (Feral et al., 2005, 2007). We now show that CD98hc absence in the epidermis *in vivo* does not phenocopy adhesion

defects as a result of β 1 epidermal loss. Because, in the skin, Src/FAK signaling acts downstream β 1 integrins (Meves et al., 2011), we investigated whether deletion of CD98hc in the epidermis affects β 1 integrin downstream signaling and, in particular, Src activation *in vivo* during wound healing (Fig. 8 A). Tail skin was wounded to obtain sufficient tissue lysate for biochemical measurements. After wounding, tail skins were freshly isolated at different time points and used to evaluate c-Src phosphorylation at tyrosine 416. During wound healing, an overall decrease in Src phosphorylation was observed in CD98hc-null epidermis compared with control skin (Fig. 8 A, pSrcY416). Src activation occurs either by dephosphorylation of Y527 or by direct competition to the binding of its SH2 domain with Y527. Thus, to investigate further how Src might be regulated, we examined Src phosphorylation on inhibitory site Y527, which revealed a similar signal between control and 4OHT skins (Fig. 8 A, pSrcY527). Instead, we found that FAK phosphorylation at Y397 is impaired in 4OHT skins compared with controls. This may explain how Src is differentially regulated during wound healing because phosphorylation of FAK on Y397 creates a very high affinity binding site for Src SH2 domain that can directly trigger Src activation (Schaller et al., 1994, 1999). Altogether, these data strengthen the idea that CD98hc acts as a modulator of integrin function *in vivo* during the early events of integrin signaling.

CD98hc deficiency induces a persistent *in vivo* activation of RhoA and its upstream activator AHRGEF12/LARG during wound healing and HF growth

Wound reepithelialization is achieved by migration of keratinocytes over the wound bed, which requires extensive remodeling of cell adhesion complexes and cell cytoskeleton. Such deep modifications at the cellular level have been associated with modulations of the activity of Rho proteins (Tscharnkte et al., 2007). This prompted us to monitor RhoA activity during epidermal wound healing in 4OHT- and vehicle-treated K14-CreER^{T2}; CD98hc^{fl/fl} mice. However, although RhoA activity has been routinely measured *in vitro* by GST-Rho binding domain (GST-RBD) pulldown assay (Ren and Schwartz, 1998), direct measurement of RhoA activity *in vivo* has rarely been reported. Here, we improved the GST-RBD pulldown assay to directly evaluate RhoA activity during *in vivo* wound closure. Whole skin from deboned tail was used; thus, contamination of the samples by dermis could not be avoided. To limit the extent of measured RhoA activity as a result of contraction of the dermal myofibroblasts, wounds were performed on the dorsum of the tail, an anatomical region which is naturally unable to contract (Falanga et al., 2004).

Before tail skin injury, RhoA activity was slightly higher in vehicle-treated K14-CreER^{T2}; CD98hc^{fl/fl} tails than in 4OHT-treated counterparts (Fig. 8 B, day 0). After epidermal wounding, in control mice, RhoA activity was transiently down-regulated at day 3 after injury and then peaked at day 5 before returning to basal levels at day 7 (Fig. 8 B, control).

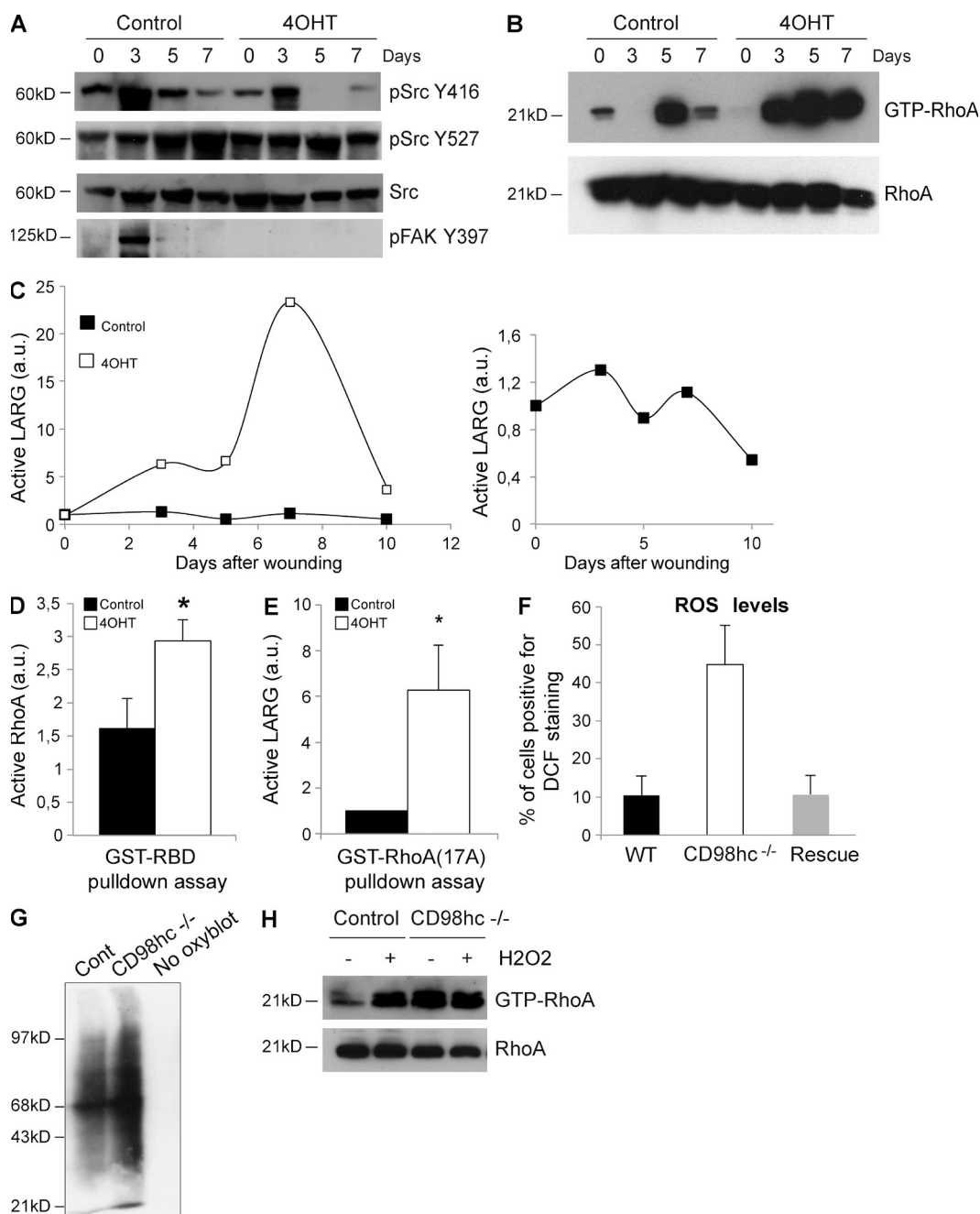


Figure 8. CD98hc is necessary for proper activation of Src and regulation of RhoA activation in vivo, during wound closure. (A) Representative Western blot analysis of pY416, pY527 Src, total Src, and p397 FAK in total skin sample lysates isolated from vehicle (control) versus 4OHT treated K14-CreER^{T2}; CD98hc^{fl/fl} mice at indicated time points after wounding. The experiment was repeated twice (two wounds per time point and per group). (B) Representative in vivo RBD assay directly measuring RhoA activity (GTP-RhoA) during wound closure from vehicle (control) versus 4OHT-treated skin of K14-CreER^{T2}; CD98hc^{fl/fl} mice at indicated time points after wounding. Total RhoA is also presented. The experiment was repeated three times (two wounds per time point and per group). (C) Quantification of in vivo AHRGEF12/LARG activity, by GST-RhoA 17A pull-down assay, in total skin sample lysates isolated from vehicle (Control) versus 4OHT-treated K14-CreER^{T2}; CD98hc^{fl/fl} mice during wound healing ($n = 2$ in each group per time point). Control only is plotted on the right. (D and E) Quantification of in vivo RhoA and AHRGEF12/LARG activities by GST-RBD and GST-RhoA 17A pull-down assay, respectively, in total skin sample lysates isolated from vehicle (control) versus 4OHT-treated K14-CreER^{T2}; CD98hc^{fl/fl} mice at dpp30 (full hair growth; $n = 6$ in each group). *, $P < 0.05$. (F) Determination of intracellular ROS levels using dichlorofluorescein (DCF), measured by flow cytometry. The percentage of positive cells is represented. Data show means of two independent experiments \pm SEM. (G) Total levels of protein oxidation were measured in vivo using Oxyblot. A representative Western blot displays one pair of mice ($n = 2$ for each group). (H) Representative in vitro RBD assay from WT (control) versus CD98hc-deficient (CD98hc^{-/-}) murine embryonic fibroblasts, pretreated (+) or not (-) with 10 μ M H₂O₂. Total RhoA is also presented.

Surprisingly, in 4OHT-treated K14-CreER^{T2}; CD98hc^{fl/fl} mice that displayed a major defect in wound healing, RhoA activity was persistently higher from days 3 to 7 after wounding, with no apparent regulation (Fig. 8 B, 4OHT).

Mechanistically, Rho proteins cycle between an active GTP-bound and an inactive GDP-bound conformation, generally upon activation or inactivation by RhoGEFs and Rho GTPase activating proteins (GAPs), respectively. Because RhoA is persistently activated during epidermal wound healing in 4OHT-treated K14-CreER^{T2}; CD98hc^{fl/fl} mice, we sought to identify its upstream active RhoGEFs during wound repair. Therefore, we performed unbiased in vivo nucleotide-free GST-RhoA 17A pulldowns on lysates from wounded mouse tails to trap and identify active RhoA-specific GEFs during wound repair (García-Mata et al., 2006; Dubash et al., 2007). In brief, GST-RhoA 17A precipitates were resolved by SDS-PAGE and differentially regulated bands were excised from the gel and analyzed by trypsin digestion coupled to LC-ESI-MS/MS. In summary, a band of an approximate size of 180 kD was identified as AHRGEF12/LARG by sequencing of seven distinct peptides (Table S3) and a band of 100 kD was identified as AHRGEF1/p115 RhoGEF by sequencing of three peptides, two of which were overlapping. To confirm the identity and regulation of those RhoGEFs, we performed nucleotide-free GST-RhoA 17A pulldowns that were analyzed by SDS-PAGE and Western blotting. Although we could not confirm p115 RhoGEF activation, we were able to detect and measure LARG activation in vivo during mouse tail epidermal wound healing. We observed that in 4OHT-treated K14-CreER^{T2}; CD98hc^{fl/fl} mice, LARG was activated to a much higher level than in control mice, up to 23-fold at day 7 after wounding (Fig. 8 C), suggesting that LARG might be responsible, at least in part, for persistent RhoA activation downstream of CD98hc during epidermal wound healing. Because p115 RhoGEF activation could not be confirmed by Western blotting in repeated experiments and was identified by only three peptides by LC-ESI-MS/MS, this would suggest, rather, that detection of p115 RhoGEF was artifactual by some means and not relevant to RhoA regulation by CD98hc during wound repair. Alternatively, we also performed, in a similar fashion, GST-RhoA 63L pulldowns to detect and identify active RhoGAPs but we were unable to detect any differentially regulated bands.

In parallel, we also assessed RhoA and LARG activation in vivo during HF growth and found that both RhoA and LARG activities were higher in 4OHT- than in vehicle-treated epidermis (Fig. 8, D and E). In conclusion, by improving the pulldown assays, we manage to reveal a striking deregulation in RhoA activity and its upstream regulator, LARG, in the absence of CD98hc during wound healing and hair growth.

CD98hc deficiency also induces amino acid transport-dependent RhoA activation via the accumulation of ROS

Besides its role of integrin signaling modulator, CD98hc can associate with specific light chains to regulate amino acid

transport. In particular, system xc⁻ is a cystine-glutamate exchange transporter composed of the xCT subunit (SLC7A11) and CD98hc. Therefore, CD98hc deficiency induces a complete loss of light chain expression at the cell surface. Expression of the xc⁻ system at the cell surface is essential for the uptake of cystine required for intracellular glutathione (GSH) synthesis, which makes it an important determinant of intracellular redox balance (Lo et al., 2008). Indeed, it turns out that ROS are direct regulators of RhoA activity, independently of any other regulatory proteins such as RhoGEFs for instance (Aghajanian et al., 2009). Therefore, we sought to assess whether CD98hc depletion could also regulate RhoA via ROS, and we used both in vitro and in vivo assays to evaluate ROS intracellular levels in CD98hc-null epidermis and relate this to RhoA activity. As a first approach, previously generated CD98hc knockout and control murine embryonic fibroblasts from CD98hc^{fl/fl} mice were stained using the redox-sensitive dye DCF-DA, followed by FACS analysis to quantify intracellular ROS levels. Approximately 45% of CD98hc KO cells showed high ROS levels, compared with 10.4% in WT controls (Fig. 8 F). Accumulation of ROS in null cells was efficiently rescued in CD98hc reconstituted null cells (10.6%; Fig. 8 F, rescue). In addition, oxidative damage to proteins (carbonyl formation) was assessed in vivo by Western blotting to measure ROS damage. ROS-mediated carbonylation of proteins in 4OHT-treated K14-CreER^{T2}; CD98hc^{fl/fl} skin was found to be sensibly higher than in vehicle-treated skin (Fig. 8 G, CD98hc^{-/-} vs. Cont), strengthening the notion that ROS levels are elevated in CD98hc-null tissues and correlated with high RhoA activity.

Finally, we assessed whether the increase of intracellular ROS had any effect on RhoA activation in WT and CD98hc-null cells by treating cell cultures with highly ROS such as hydrogen peroxide (Fig. 8 H). As expected, treatment with 10 μ M hydrogen peroxide for 10 min triggered RhoA activation in control cells. In contrast, in CD98hc-null cells, in which basal RhoA activity was already equivalent to that of H₂O₂-treated controls, H₂O₂ treatment was ineffective, suggesting that, in these cells, ROS levels were already at their maximal level. Collectively, these results demonstrate that the sustained in vivo activation of RhoA in CD98hc-null cells is mediated by both RhoGEF regulation, most likely via CD98hc-dependent integrin signaling, and by intracellular accumulation of ROS caused by an amino acid transport defect.

DISCUSSION

CD98hc expression, first reported in both basal keratinocytes (Patterson et al., 1984) and HF epithelium (Fernández-Herrera et al., 1989), was then correlated to cell proliferation in epidermis and several other epithelial tissues (Devés and Boyd, 2000). Although studies of cultured keratinocytes have concluded that CD98hc is an important regulator of keratinocyte adhesion and differentiation (Lemaître et al., 2011), its possible role in epidermal homeostasis in vivo remains an open question. Using young adult mice, we show here that CD98hc sustains hair regeneration and efficient wound healing by

maintaining basal keratinocyte *in vivo* functions as crucial as cell proliferation and migration. These defects evoke age-related alterations. Consistently, CD98hc expression level is reduced in elderly murine and human skin similarly to epidermal $\beta 1$ integrin, strongly suggesting that CD98hc itself could participate in changes associated with aging. Although deletion of CD98hc in the epidermis *in vivo* has no effect on cell adhesion, its deficiency decreases Src activation (Tyr416) and induces a sustained RhoA activation, along with strong activation of the Rho GEF LARG, during epidermal homeostasis and wound repair in young mice. We also show that impaired amino acid transport caused by the absence of CD98hc is involved in sustained RhoA activation *in vivo*. Altogether, our results clarify the role of CD98hc in the integument *in vivo* and unveil novel unsuspected functions in basal keratinocyte biology during aging.

Although human cultured keratinocytes were reported to depend on CD98hc to regulate cell adhesion and differentiation *in vitro* (Lemaître et al., 2011), our data clearly show that CD98hc-deficient keratinocytes preserve their adhesion capacity both *in vivo* in the murine epidermis and *in vitro* in mouse primary keratinocytes. The discrepancy of cell adhesion behavior *in vitro* can be explained by the fact that, although we used homologous recombination deletion of CD98hc *in vivo*, followed by primary keratinocyte isolation and culture, Lemaître et al. (2011) performed their experiments on cultured human keratinocytes, isolated from neonatal foreskin and nucleofected with specific CD98hc shRNA. Both cell provenance and gene invalidation techniques used could explain this apparent divergence. Despite these studies on human cultured keratinocytes, our data clearly indicate that CD98hc is dispensable for cell adhesion *in vivo*.

Similarly, and although CD98hc binds $\beta 1$ integrin, CD98hc absence in the epidermis does not phenocopy $\beta 1$ epidermal deletion, in particular skin blistering. Our results suggest that *in vivo* CD98hc is expandable to $\beta 1$ integrin activation in the epidermis, which makes CD98hc unnecessary to cell adhesion *in vivo*. Expression levels of integrins are also maintained in the absence of CD98hc in basal keratinocytes. Altogether these results are in good agreement with our previous *in vitro* data on embryonic stem cell-derived fibroblasts. Thus, our data identify CD98hc as a relevant integrin signaling mediator in the epidermis *in vivo*, rather than a $\beta 1$ integrin-dependent cell adhesion regulator as shown *in vitro* on cultured human keratinocytes (Lemaître et al., 2011). Our data also suggest that during wound closure, CD98hc, which is involved in integrin outside-in signaling, participates in Src activation and regulation of RhoA. These results reinforce the concept by which CD98hc is a significant integrin signaling mediator in the epidermis *in vivo*.

Changes induced by skin aging are associated with reduced expression of $\beta 1$ integrin. Previous studies seem to indicate that this progressive expression decrease alters epidermis via defects in integrin signaling rather than cell adhesion (Bosset et al., 2003; Giangreco et al., 2010). Our data showing a similar reduction of CD98hc expression during aging strengthen

this notion even further and suggest that CD98hc itself could participate in aging via its role as integrin signaling modulator. Thus, CD98hc status *in vivo* could be an indicator of the capacity of the skin to regenerate.

Remodeling of cell adhesion complexes and cytoskeleton is essential for migration of keratinocytes during epidermal repair. This requires an appropriate regulation of Rho GTPases (Tscharntke et al., 2007). Moreover, Rac1 deletion in basal keratinocytes induces defects in HF organization and HF cycle, pointing out a general role for small GTPases in the regulation of cell behavior during both tissue homeostasis and repair (Benitah et al., 2005; Chrostek et al., 2006). In light of the phenotype expressed by the selectively deleted CD98hc mice, *in vivo* integrin-dependent signals that support cell migration during hair growth and wound closure were investigated. Direct assessment of RhoA activity during wound healing required improvement of the classical GST-RBD pulldown assay and adaptation to *in vivo* conditions. Indeed, *in vivo* studies on Rho GTPases have usually been performed using murine transgenic dominant-negative or full knockout models (Tscharntke et al., 2007), which provides physiologically limited information because these approaches may affect intrinsic Rho protein regulation (Boulter et al., 2010). In contrast, in our case, RhoA activity was measured *in vivo* without altering the intrinsic physiology of the animal model.

Interestingly, in agreement with mechanisms described for collective cell migration (Ilna and Friedl, 2009), we show that RhoA is persistently activated in the absence of CD98hc during both wound closure and HF growth. We identified, from biochemical experiments performed on mice, AHRGEF12/LARG and AHRGEF1/p115 RhoGEF as the RhoGEFs activated in the absence of CD98hc. However, only LARG activation could be confirmed by Western blotting. LARG and p115 RhoGEF, together with PDZ RhoGEF, are members of the RGS-GEF family of RhoGEFs. These GEFs have a classical DH-PH tandem domain that regulates nucleotide exchange on Rho proteins as well as an N-terminal RGS domain which enables their regulation by GPCRs (Suzuki et al., 2003; Rossman et al., 2005). Indeed, LARG has been established as one of the GEFs responsible for RhoA activation downstream of integrin ligation to fibronectin (Dubash et al., 2007), and it is therefore not surprising that we find it regulated upon loss of CD98hc, a crucial regulator of integrin signaling. Nevertheless, at this point, we do not know how CD98hc regulates LARG. It was recently shown that Fyn may stimulate LARG activity downstream of integrins (Guilluy et al., 2011), but we observe, rather, an inhibition of Src family kinases upon loss of CD98hc in our experimental model, which suggests that LARG has to be activated by other means. These may possibly include phosphorylation by kinases such as PKC α or FAK, for instance (Chikumi et al., 2002; Disatnik et al., 2002; Suzuki et al., 2003; Dovas et al., 2006), as well as regulation of LARG homodimerization by CD98hc, which has long been known to regulate its activity (Chikumi et al., 2004). Further molecular investigations, *in vitro*, in cell culture should be performed to dissect this regulation. Regarding

p115 RhoGEF, we were unable to confirm its activation by Western blotting and, therefore, we would refrain from drawing any conclusion on its regulation by CD98hc. More surprising, however, might be the fact that we did not find any RhoGAP differentially regulated, especially given RhoA overactivation and the regulation of several of them by integrins and cell adhesion (Arthur et al., 2000; Arthur and Burridge, 2001). Nevertheless, GST-RhoA 63L pulldown assays are designed to detect and measure active RhoGAPs (or increased activity) and, therefore, we cannot exclude the possibility that some RhoGAPs might be inactivated to and from levels that cannot be detected with that assay. Incidentally, inactivation of RhoGAPs would further strengthen RhoA activation.

A recent work on yolk syncytial layer formation in zebrafish embryo shows that loss of CD98hc induces inhibition of Src and triggers the activation of RhoA (Takesono et al., 2012). The authors speculate that this specific regulation of RhoA would occur via the regulation of p190 RhoGAP by Src. Although our results show a similar effect of loss of CD98hc on Src phosphorylation and RhoA activation in the epidermis, we did not detect any inhibition of p190 RhoGAP using GST-RhoA 63L pulldown assays and were unable to unequivocally conclude on p190 RhoGAP regulation downstream of CD98hc. Nevertheless, this and the activation of RhoA by LARG do not preclude an effect of loss of CD98hc on p190 RhoGAP as well. Our data, together with Takesono's studies (Takesono et al., 2012), support the idea that the CD98–integrin–Src–RhoA signaling pathway may play an evolutionary well conserved and pivotal role in tissue development and homeostasis. In conclusion, similarly to Livshits et al. (2012), we now show that not only Rho protein activity (RhoA and Rac1, respectively) but also RhoGEF activity can be measured biochemically in vivo during both skin homeostasis and repair. Additionally, we show that loss of CD98hc induces an aberrant regulation of RhoA activity, most likely via its RhoGEF LARG, during wound closure and HF growth, two integrin-dependent biological processes.

Loss of CD98hc in the skin also highlights an atypical regulation of RhoA by ROS as the result of a defect in amino acid transport induced by CD98hc deletion. Besides the activation of the RhoA-specific GEF LARG during both hair growth and wound healing in vivo, we provide data clearly indicating that defects in CD98hc/xCT amino acid transport also participate in persistent RhoA activation. This RhoGEF-independent modulation of RhoA does not impede its regulation by LARG at the same time but highlights a role for both functions of CD98hc (amino acid transporter and integrin signaling modulator) in epidermal homeostasis in vivo via the regulation of the small G protein RhoA.

Young mice epidermis presents an early boost of proliferation, with rapid tissue renewal cycles, in particular during the first synchronous hair growth of adult life. Along with skin aging, epidermis renewal slows down (Giangreco et al., 2008). The selective effect of CD98hc deletion on young versus old epidermis strongly suggests that CD98hc is required for a

massive and efficient contribution in skin homeostasis, in particular in the situation of high epidermal renewal phase (hair growth and wound healing). Indeed, in light of our results, CD98hc appears to be not a mere marker for epidermal proliferative keratinocytes (Lemaître et al., 2005) but a crucial actor in skin homeostasis endowed with defined intrinsic functions. Our data, which are in agreement with previous studies showing dependence on CD98hc for proliferation of nonepithelial cells (Cantor et al., 2009; Fogelstrand et al., 2009), further widen the notion that CD98hc expression provides cells with a profound selective advantage.

One implication of our work relates to the self-renewal of mammalian epithelia. CD98hc is highly expressed on the surface of epithelial cells of most embryonic and adult tissues, including epidermis, the choroid plexus in the brain and retina, and in intestinal, renal, and thymic epithelium (Nakamura et al., 1999; Rossier et al., 1999; Dave et al., 2004). CD98hc overexpression in intestinal epithelial cells induces gut homeostatic defects linked to changes in cell proliferation and survival consequent to integrin signaling alterations (Nguyen et al., 2011). We now clearly demonstrate a crucial role for CD98hc in maintaining basal keratinocyte functions throughout the epidermis, including IFE and HF, via its ability to mediate integrin signaling. Because most of the human malignancies arise in actively self-renovating sites of epithelial tissues (Sen et al., 2010), integrin signaling is thought to play an important role in formation and maintenance of epithelial cancers (White et al., 2004; Kass et al., 2007). Considering the physiological role of CD98hc in mammalian epithelial tissue formation and homeostasis, and the fact that enhanced expression of CD98hc epithelial neoplasias is indicative of malignant evolution (Cantor and Ginsberg, 2012), it could be hypothesized that novel studies on such a multifunctional protein would pave the way to new discoveries.

MATERIALS AND METHODS

Mice. All procedures were approved by the Institutional Animal Care and Use Committee at the University of Nice-Sophia Antipolis, Nice, France. CD98hc conditional null mice, *CD98hc^{fl/fl}* (Féral et al., 2007), were crossed with *K14-CreER^{T2}* transgenic mice (gift of B. Stripp, Duke University Medical Center, Durham, NC; Hong et al., 2004). Mixed background C57BL/6-svj129 *K14CreER^{T2}*; *CD98hc^{fl/fl}* mice have been backcrossed seven times onto the C57BL/6 backgrounds. All experiments were performed on both backgrounds (mixed and pure C57BL/6). For all in vivo and ex vivo experiments, *K14CreER^{T2}*; *CD98hc^{fl/fl}* mice and age-matched *CD98hc^{fl/fl}* littermate controls were used. To induce CD98hc deletion, mice were treated topically six times once a day every other day with 1.5 mg 4OHT (Sigma-Aldrich) on tails or shaved back skin. Importantly, mice were weaned at dpp19, when the first 4OHT treatment occurred. 4OHT was dissolved either in acetone or ethanol 100% without any noticeable effect.

Genomic DNA PCR. Genomic DNA was isolated from dermis, epidermis, or cultured keratinocytes by 1-h incubation at 100°C in 50 μ l NaOH solution (25 mM NaOH/2 mM EDTA), followed by neutralization with 50 μ l Tris Solution (40 mM Tris-HCl). 100–500 ng of genomic DNA was used for PCR reactions using primers reported in Table S1. Primer pairs A/B allowed detection of WT and floxed allele (248 and 304 bp, respectively). CD98hc deletion was detected using A/F primers (recombinant allele 386 bp). Transgene K14CreER was detected by primers C/D (268 bp).

In vivo wound healing. 10 d after the last 4OHT treatment, mice were anesthetized by intraperitoneal injection of rodent cocktail (0.015 mg xylazine/0.075 mg ketamine per gram of body weight). A full thickness wound was made using a dermal biopsy 5-mm punch on the back of shaved mice. Pictures were taken at days 0, 3, 5, 7, and 10 and used for wound area quantification. Mice were sacrificed at various time points during healing ($n \geq 3$ per time point). Samples for paraffin-embedded and frozen processing were collected from the wounded area and the surrounding skin.

For tail wounding experiments, a week after the last 4OHT treatment, mice were anesthetized (see above). Mouse tail was partially excised using a blood lancet (23G) and four wounds were made at perpendicular angles on the entire length of the tail. Mice were sacrificed at various time points and tails were harvested.

To examine rounding of skin $\gamma\delta$ T cells at the wound site, full-thickness wounds were generated in ears from K14-CreERT2; CD98hcf1/fl mice (4OHT- or vehicle-treated) using a 2-mm punch tool, and wounded tissue was harvested 2 h later. Wounded ears were excised, peeled into halves, digested in 2 U/ml dispase II (Sigma-Aldrich) for 40 min, and fixed in 2% paraformaldehyde. Epidermal sheets were stained with PE-conjugated anti- $\gamma\delta$ TCR (GL3eBioscience).

Histology and immunohistochemistry. Tissue samples (4- μ m frozen sections and 7- μ m paraffin-embedded sections) were processed and prepared for standard histological and immunohistochemical procedures (Estrach et al., 2006). Formalin-fixed paraffin sections were used for all histology except for CD98, Ki67, $\alpha 6$, and $\beta 1$ integrins and laminin 332 immunostaining, which were performed on frozen sections. Antibodies were: rabbit anti-mouse involucrin (Covance), rabbit anti-mouse cytokeratin 10 (Covance), goat anti-mouse Ki67 (M-19; Santa Cruz Biotechnology, Inc.), rat anti-integrin $\beta 1$ (MAB1997; Millipore), monoclonal anti- $\alpha 6$ (GoH3; R&D Systems), rabbit anti-laminin 332 (SE144, gift of L. Gagnoux-Palacios, Institut National de la Sante et de la Recherche Medicale U634, Nice, France; Vailly et al., 1994), rat anti-mouse CD98 (clone RL388; eBioscience), rat anti-mouse macrophage Mac 2 (clone CL8942 AP; Cedarlane), rat IgG2a isotype control (eBioscience), and Alexa Fluor 488- or 546-conjugated anti-rat, -mouse, -goat, or -rabbit (Invitrogen).

qPCR/RNA preparation. RNAs were extracted from back skin samples using TRIzol reagent (Gibco). Reverse transcription was performed on total RNA using Superscript II reverse transcription (Invitrogen) according to the manufacturer's instructions. Sets of specific primers (Table S2) were used for amplification using the 7900HT Real Time PCR System (Applied Biosystems). Samples were normalized to GAPDH using the Δ Ct method. Statistical significance was determined with Student's *t* test.

Flow cytometry. Immunolabeled cells were analyzed on a flow cytometer (FACSCalibur; BD) with CellQuest software (BD). Preparation and staining of single cell suspension from adult epidermis were performed as described elsewhere (Nowak and Fuchs, 2009). Antibodies were anti- $\beta 1$ (9EG7; BD) and anti- $\beta 4$ (346-11A; BD), both used according to the manufacturers' recommendations.

Cell culture. Primary mouse keratinocytes were isolated from K14CreERT2; CD98hcf1/fl young adult skin as previously described (Jensen et al., 2010). CFE assays were performed as previously described (Jensen et al., 2010).

Adhesion and migration/wound in vitro. Cell adhesion was measured using freshly isolated primary keratinocytes, as previously described, using type I collagen as ECM. Primary keratinocytes were plated in complete FAD medium without calcium (Jensen et al., 2010) and in the absence of feeders. The adhesion was monitored by live imaging and then scored. Cell scratching was performed using a scarificator, which was previously described by Turchi et al. (2002). In classical conditions, 40–50% of the cell culture was scratched and the width between the wound edges was \sim 300–400 μ m. Cells were plated in complete FAD medium without calcium, in the absence of feeders and treated with 4OHT (200 nM in DMSO) or DMSO only 72 h before scratching.

GST-RBD and GST-RhoA 17A pulldown assays. RhoA activity was measured using a modified GST-RBD assay (Ren et al., 1999). In brief, mouse tails were harvested at the indicated days after wounding, deboned, and snap frozen in liquid nitrogen. For hair growth samples, back skin from mice at dpp30 was isolated and snap frozen. All murine samples were crushed in liquid nitrogen and thawed for 10 min in 50 mM Hepes, pH 7.4, 250 mM NaCl, 5 mM MgCl₂, 1% Triton X-100, 0.1% SDS, 5 mM dithiothreitol (DTT), and mini EDTA-free protease inhibitors (Roche) at 4°C. Tissues were homogenized using a mechanical homogenizer for 10 s. Insoluble material was removed by centrifugation for 10 min at 9,500 g and lysates were incubated for 40 min with 50 μ g of immobilized GST-RBD to measure RhoA activity. Alternatively, to measure RhoA activity in cells, cells were lysed in the same buffer and cell lysates processed similarly.

Active RhoGEFs were trapped using a modified nucleotide-free GST-RhoA 17A pulldown assay (García-Mata et al., 2006). In brief, mouse tails were harvested at the indicated days after wounding, deboned, and snap frozen in liquid nitrogen. Murine samples were crushed in liquid nitrogen and thawed for 10 min in 50 mM Hepes, pH 7.4, 250 mM NaCl, 5 mM MgCl₂, 1% Triton X-100, 0.1% SDS, 5 mM DTT, 10 mM NaF, and mini EDTA-free protease inhibitors (Roche) at 4°C. Tissues were homogenized using a mechanical homogenizer for 10 s. Insoluble material was removed by centrifugation for 10 min at 9,500 g and lysates were incubated for 40 min with 50 μ g of immobilized GST-RhoA 17A to measure RhoGEF activity. Alternatively, cells were lysed in 20 mM Hepes, pH 7.4, 150 mM NaCl, 5 mM MgCl₂, 1% Triton X-100, 1 mM DTT, 10 mM NaF, and mini EDTA-free protease inhibitors (Roche) at 4°C. Cell lysates were then processed as mentioned previously.

LC-ESI-MSMS protein identification. Protein identification was performed by Eurogentec. In brief, the analysis was performed on an LC (nona Ultimate 3000; Dionex)-ESI-ion trap (AMAZONE-Bruker), in positive mode. The samples were excised from 1D SDS-PAGE, reduced, alkylated, and digested in gel using trypsin. The peptide digests obtained were analyzed independently by LC-ESI-MSMS. Spectra were treated using Data analysis (version 3.0; Bruker). Databases searches were done on Protein Scape (Bruker) using xml, which was generated using the Compass AutomationEngine utilities (Bruker). The search was performed using the SwissProt database restricted to the *Mus musculus* taxonomy.

Western blotting. SDS-PAGE and Western blots were performed as described in Boulter et al. (2010). Anti-pSrc Y527, pSrc Y416, Src (36D10), and pFAK Y397 antibodies were from Cell Signaling Technology. The anti-RhoA 26C4 antibody was from Santa Cruz Biotechnology, Inc.

ROS level measurements. ROS intracellular levels were measured using DCF-DA (Invitrogen). In brief, cells were plated and cultured in normal conditions. 48 h after plating, cells were washed once with HBSS, incubated with 1 μ M DCF-DA for 30 min at 37°C, and then harvested, washed in HBSS, and levels of intracellular fluorescence analyzed using a FACSCalibur (BD). For RhoA activity assessment, cells were plated and treated with 10 μ M H₂O₂ for 10 min before performing the GST-RBD assay as previously described.

Protein carbonyl assay in vivo. Mouse back skins were harvested and snap frozen in liquid nitrogen. Murine samples were crushed in liquid nitrogen and thawed for 10 min in 50 mM Hepes, pH 7.4, 250 mM NaCl, 5 mM MgCl₂, 1% Triton X-100, 0.1% SDS, 5 mM DTT, and mini EDTA-free protease inhibitors (Roche) at 4°C. Supernatants were assayed for protein content (BCA; Pierce) and 100 μ g protein was assayed for protein carbonyls as per the manufacturer's instructions (OxyBlot; Millipore).

Microscope image acquisition. The samples were observed using either Axiophot (epifluorescence; Carl Zeiss), or DM 4000B (histology; Leica), Axiovert 200M (live imaging; Carl Zeiss), or an LSM 5 EXCITER confocal microscope (dendritic epidermal T cell staining; Carl Zeiss). The objectives

used in this study were: for the AxioPhot, Objective Plan Neofluar 20×/0.5 and Plan Achromat objective 40×/0.95; for the DM4000, objective 20× PH2/0.50 and objective 40× PH2/0.75; for the Axiovert, objective 5×/0.12; and for the LSM 5 EXCITER, objective Plan Neofluar 20×/0.5. On fixed samples, all the acquisitions were performed at room temperature; for live imaging, experiments were performed at 37°C under 5% CO₂. The mounting media used were PermaFluor Aqueous Medium (Thermo Fisher Scientific) and Mountex, nonaqueous (Histolab; MicroTech). The fluorochromes used were Alexa Fluor–coupled secondary antibodies (488/594). The images were acquired using, respectively, AxioCam MRm (Carl Zeiss), DFC 425C (Leica), and cool snap cameras (Hamamatsu Photonics) and the software for acquisition were, respectively, AxioVision, Leica application suite version 3.8, ZEN V2009, and MetaMorph.

Online supplemental material. Table S1 shows a genotyping primer list. Table S2 shows quantitative PCR primers. Table S3 shows LC-ESI-MSMS protein identification. Online supplemental material is available at <http://www.jem.org/cgi/content/full/jem.20121651/DC1>.

We thank A. Loubat for technical help, Institut National de la Santé et de la Recherche Médicale (INSERM) U634 members for comments, and M.H. Ginsberg (University of California, San Diego) for useful discussion and support regarding transferring CD98hc^{fl/fl} mice. We also acknowledge G. Ponzio (Institut de Pharmacologie Moléculaire et Cellulaire, Sophia-Antipolis) for the use of the cells' scarificator.

This study was supported by grants from INSERM InCa/AVENIR (R08227AS), from Association pour la Recherche sur le Cancer (ARC N3179), and from Agence Nationale de la Recherche (ANR R09101AS). E. Boulter was the recipient of a postdoctoral fellowship from the Ligue Nationale Contre le Cancer (RAB 12007 ASA) and a Marie Curie International Reintegration Grant from the European Union seventh Framework Program under the agreement 276945.

The authors declare no competing financial interests

Author Contributions: E. Boulter, S. Estrach, and C.C. Féral developed study concept and design. A. Errante maintained murine colonies, including performing mice genotyping, and carried out most treatments on [K14CreER²;CD98hc^{fl/fl}] mice. F. Tissot and C. Pons performed the histological and immunofluorescent staining of mice sections, under the supervision of C.C. Féral, who performed the analysis and quantification of these samples. C.C. Féral performed the wound healing experiments in vivo with the technical help of A. Errante and C. Pons. S. Estrach trained C.C. Féral and E. Boulter for isolation and culturing primary keratinocytes and performed and analyzed all qPCR experiments and ROS study on murine samples. L. Cailleteau performed most FACS analysis. E. Boulter performed all cell migration assays and biochemical studies both in vivo and in vitro. G. Meneguzzi gave input to interpretation and manuscript preparation. E. Boulter, S. Estrach, and C.C. Féral wrote the manuscript.

Submitted: 24 July 2012

Accepted: 7 December 2012

REFERENCES

- Aghajanian, A., E.S. Wittchen, S.L. Campbell, and K. Burridge. 2009. Direct activation of RhoA by reactive oxygen species requires a redox-sensitive motif. *PLoS ONE*. 4:e8045. <http://dx.doi.org/10.1371/journal.pone.0008045>
- Alonso, L., and E. Fuchs. 2006. The hair cycle. *J. Cell Sci.* 119:391–393. <http://dx.doi.org/10.1242/jcs.02793>
- Arthur, W.T., and K. Burridge. 2001. RhoA inactivation by p190RhoGAP regulates cell spreading and migration by promoting membrane protrusion and polarity. *Mol. Biol. Cell.* 12:2711–2720.
- Arthur, W.T., L.A. Petch, and K. Burridge. 2000. Integrin engagement suppresses RhoA activity via a c-Src-dependent mechanism. *Curr. Biol.* 10:719–722. [http://dx.doi.org/10.1016/S0960-9822\(00\)00537-6](http://dx.doi.org/10.1016/S0960-9822(00)00537-6)
- Benitah, S.A., M. Frye, M. Glogauer, and F.M. Watt. 2005. Stem cell depletion through epidermal deletion of Rac1. *Science*. 309:933–935. <http://dx.doi.org/10.1126/science.1113579>
- Blanpain, C., and E. Fuchs. 2009. Epidermal homeostasis: a balancing act of stem cells in the skin. *Nat. Rev. Mol. Cell Biol.* 10:207–217. <http://dx.doi.org/10.1038/nrm2636>
- Bosset, S., M. Bonnet-Duquennoy, P. Barré, A. Chalou, K. Lazou, R. Kurfurst, F. Bonté, S. Schnébert, F. Disant, B. Le Varlet, and J.F. Nicolas. 2003. Decreased expression of keratinocyte beta1 integrins in chronically sun-exposed skin in vivo. *Br. J. Dermatol.* 148:770–778. <http://dx.doi.org/10.1046/j.1365-2133.2003.05159.x>
- Boulter, E., R. Garcia-Mata, C. Guilluy, A. Dubash, G. Rossi, P.J. Brennwald, and K. Burridge. 2010. Regulation of Rho GTPase cross-talk, degradation and activity by RhoGD11. *Nat. Cell Biol.* 12:477–483. <http://dx.doi.org/10.1038/ncb2049>
- Brakebusch, C., R. Grose, F. Quondamatteo, A. Ramirez, J.L. Jorcano, A. Pirro, M. Svensson, R. Herken, T. Sasaki, R. Timpl, et al. 2000. Skin and hair follicle integrity is crucially dependent on beta 1 integrin expression on keratinocytes. *EMBO J.* 19:3990–4003. <http://dx.doi.org/10.1093/emboj/19.15.3990>
- Cantor, J.M., and M.H. Ginsberg. 2012. CD98 at the crossroads of adaptive immunity and cancer. *J. Cell Sci.* 125:1373–1382. <http://dx.doi.org/10.1242/jcs.096040>
- Cantor, J., C.D. Browne, R. Ruppert, C.C. Féral, R. Fässler, R.C. Rickert, and M.H. Ginsberg. 2009. CD98hc facilitates B cell proliferation and adaptive humoral immunity. *Nat. Immunol.* 10:412–419. <http://dx.doi.org/10.1038/ni.1712>
- Chandrasekaran, S., N.H. Guo, R.G. Rodrigues, J. Kaiser, and D.D. Roberts. 1999. Pro-adhesive and chemotactic activities of thrombospondin-1 for breast carcinoma cells are mediated by alpha3beta1 integrin and regulated by insulin-like growth factor-1 and CD98. *J. Biol. Chem.* 274:11408–11416. <http://dx.doi.org/10.1074/jbc.274.16.11408>
- Chikumi, H., S. Fukuhara, and J.S. Gutkind. 2002. Regulation of G protein-linked guanine nucleotide exchange factors for Rho, PDZ-RhoGEF, and LARG by tyrosine phosphorylation: evidence of a role for focal adhesion kinase. *J. Biol. Chem.* 277:12463–12473. <http://dx.doi.org/10.1074/jbc.M108504200>
- Chikumi, H., A. Barac, B. Behbahani, Y. Gao, H. Teramoto, Y. Zheng, and J.S. Gutkind. 2004. Homo- and hetero-oligomerization of PDZ-RhoGEF, LARG and p115RhoGEF by their C-terminal region regulates their in vivo Rho GEF activity and transforming potential. *Oncogene*. 23:233–240. <http://dx.doi.org/10.1038/sj.onc.1207012>
- Chrostek, A., X. Wu, F. Quondamatteo, R. Hu, A. Sanecka, C. Niemann, L. Langbein, I. Haase, and C. Brakebusch. 2006. Rac1 is crucial for hair follicle integrity but is not essential for maintenance of the epidermis. *Mol. Cell Biol.* 26:6957–6970. <http://dx.doi.org/10.1128/MCB.00075-06>
- Clayton, E., D.P. Doupé, A.M. Klein, D.J. Winton, B.D. Simons, and P.H. Jones. 2007. A single type of progenitor cell maintains normal epidermis. *Nature*. 446:185–189. <http://dx.doi.org/10.1038/nature05574>
- Dave, M.H., N. Schulz, M. Zecevic, C.A. Wagner, and F. Verrey. 2004. Expression of heteromeric amino acid transporters along the murine intestine. *J. Physiol.* 558:597–610. <http://dx.doi.org/10.1113/jphysiol.2004.065037>
- Devés, R., and C.A. Boyd. 2000. Surface antigen CD98(4F2): not a single membrane protein, but a family of proteins with multiple functions. *J. Membr. Biol.* 173:165–177. <http://dx.doi.org/10.1007/s002320001017>
- Disatnik, M.H., S.C. Boutet, C.H. Lee, D. Mochly-Rosen, and T.A. Rando. 2002. Sequential activation of individual PKC isozymes in integrin-mediated muscle cell spreading: a role for MARCKS in an integrin signaling pathway. *J. Cell Sci.* 115:2151–2163.
- Dovas, A., A. Yoneda, and J.R. Couchman. 2006. PKCbeta-dependent activation of RhoA by syndecan-4 during focal adhesion formation. *J. Cell Sci.* 119:2837–2846. <http://dx.doi.org/10.1242/jcs.03020>
- Dubash, A.D., K. Wennerberg, R. Garcia-Mata, M.M. Menold, W.T. Arthur, and K. Burridge. 2007. A novel role for Lsc/p115 RhoGEF and LARG in regulating RhoA activity downstream of adhesion to fibronectin. *J. Cell Sci.* 120:3989–3998. <http://dx.doi.org/10.1242/jcs.003806>
- Estrach, S., C.A. Ambler, C. Lo Celso, K. Hozumi, and F.M. Watt. 2006. Jagged 1 is a beta-catenin target gene required for ectopic hair follicle formation in adult epidermis. *Development*. 133:4427–4438. <http://dx.doi.org/10.1242/dev.02644>
- Falanga, V., D. Schryer, J. Cha, J. Butmarc, P. Carson, A.B. Roberts, and S.J. Kim. 2004. Full-thickness wounding of the mouse tail as a model for delayed wound healing: accelerated wound closure in Smad3 knock-out

- mice. *Wound Repair Regen.* 12:320–326. <http://dx.doi.org/10.1111/j.1067-1927.2004.012316.x>
- Fenczik, C.A., T. Sethi, J.W. Ramos, P.E. Hughes, and M.H. Ginsberg. 1997. Complementation of dominant suppression implicates CD98 in integrin activation. *Nature.* 390:81–85. <http://dx.doi.org/10.1038/36349>
- Fenczik, C.A., R. Zent, M. Dellos, D.A. Calderwood, J. Satriano, C. Kelly, and M.H. Ginsberg. 2001. Distinct domains of CD98hc regulate integrins and amino acid transport. *J. Biol. Chem.* 276:8746–8752. <http://dx.doi.org/10.1074/jbc.M011239200>
- Feral, C.C., N. Nishiya, C.A. Fenczik, H. Stuhlmann, M. Slepak, and M.H. Ginsberg. 2005. CD98hc (SLC3A2) mediates integrin signaling. *Proc. Natl. Acad. Sci. USA.* 102:355–360. <http://dx.doi.org/10.1073/pnas.0404852102>
- Féral, C.C., A. Zijlstra, E. Tkachenko, G. Prager, M.L. Gardel, M. Slepak, and M.H. Ginsberg. 2007. CD98hc (SLC3A2) participates in fibronectin matrix assembly by mediating integrin signaling. *J. Cell Biol.* 178:701–711. <http://dx.doi.org/10.1083/jcb.200705090>
- Fernández-Herrera, J., F. Sánchez-Madrid, and A.G. Díez. 1989. Differential expression of the 4F2 activation antigen on human follicular epithelium in hair cycle. *J. Invest. Dermatol.* 92:247–250. <http://dx.doi.org/10.1111/1523-1747.ep12276789>
- Fogelstrand, P., C.C. Féral, R. Zargham, and M.H. Ginsberg. 2009. Dependence of proliferative vascular smooth muscle cells on CD98hc (4F2hc, SLC3A2). *J. Exp. Med.* 206:2397–2406. <http://dx.doi.org/10.1084/jem.20082845>
- García-Mata, R., K. Wennerberg, W.T. Arthur, N.K. Noren, S.M. Ellerbroek, and K. Burridge. 2006. Analysis of activated GAPs and GEFs in cell lysates. *Methods Enzymol.* 406:425–437. [http://dx.doi.org/10.1016/S0076-6879\(06\)06031-9](http://dx.doi.org/10.1016/S0076-6879(06)06031-9)
- Giangreco, A., M. Qin, J.E. Pintar, and F.M. Watt. 2008. Epidermal stem cells are retained in vivo throughout skin aging. *Aging Cell.* 7:250–259. <http://dx.doi.org/10.1111/j.1474-9726.2008.00372.x>
- Giangreco, A., S.J. Goldie, V. Failla, G. Saintigny, and F.M. Watt. 2010. Human skin aging is associated with reduced expression of the stem cell markers beta1 integrin and MCSP. *J. Invest. Dermatol.* 130:604–608. <http://dx.doi.org/10.1038/jid.2009.297>
- Gosain, A., and L.A. DiPietro. 2004. Aging and wound healing. *World J. Surg.* 28:321–326. <http://dx.doi.org/10.1007/s00268-003-7397-6>
- Grose, R., C. Hutter, W. Bloch, I. Thorey, F.M. Watt, R. Fässler, C. Brakebusch, and S. Werner. 2002. A crucial role of beta 1 integrins for keratinocyte migration in vitro and during cutaneous wound repair. *Development.* 129:2303–2315.
- Guilluy, C., V. Swaminathan, R. Garcia-Mata, E.T. O'Brien, R. Superfine, and K. Burridge. 2011. The Rho GEFs LARG and GEF-H1 regulate the mechanical response to force on integrins. *Nat. Cell Biol.* 13:722–727. <http://dx.doi.org/10.1038/ncb2254>
- Henderson, N.C., E.A. Collis, A.C. Mackinnon, K.J. Simpson, C. Haslett, R. Zent, M. Ginsberg, and T. Sethi. 2004. CD98hc (SLC3A2) interaction with beta 1 integrins is required for transformation. *J. Biol. Chem.* 279:54731–54741. <http://dx.doi.org/10.1074/jbc.M408700200>
- Hong, K.U., S.D. Reynolds, S. Watkins, E. Fuchs, and B.R. Stripp. 2004. Basal cells are a multipotent progenitor capable of renewing the bronchial epithelium. *Am. J. Pathol.* 164:577–588. [http://dx.doi.org/10.1016/S0002-9440\(10\)63147-1](http://dx.doi.org/10.1016/S0002-9440(10)63147-1)
- Iлина, O., and P. Friedl. 2009. Mechanisms of collective cell migration at a glance. *J. Cell Sci.* 122:3203–3208. <http://dx.doi.org/10.1242/jcs.036525>
- Ito, M., Y. Liu, Z. Yang, J. Nguyen, F. Liang, R.J. Morris, and G. Cotsarelis. 2005. Stem cells in the hair follicle bulge contribute to wound repair but not to homeostasis of the epidermis. *Nat. Med.* 11:1351–1354. <http://dx.doi.org/10.1038/nm1328>
- Jensen, K.B., R.R. Driskell, and F.M. Watt. 2010. Assaying proliferation and differentiation capacity of stem cells using disaggregated adult mouse epidermis. *Nat. Protoc.* 5:898–911. <http://dx.doi.org/10.1038/nprot.2010.39>
- Jones, P.H., and F.M. Watt. 1993. Separation of human epidermal stem cells from transit amplifying cells on the basis of differences in integrin function and expression. *Cell.* 73:713–724. [http://dx.doi.org/10.1016/0092-8674\(93\)90251-K](http://dx.doi.org/10.1016/0092-8674(93)90251-K)
- Kass, L., J.T. Erler, M. Dembo, and V.M. Weaver. 2007. Mammary epithelial cell: influence of extracellular matrix composition and organization during development and tumorigenesis. *Int. J. Biochem. Cell Biol.* 39:1987–1994. <http://dx.doi.org/10.1016/j.biocel.2007.06.025>
- Kolesnikova, T.V., B.A. Mannion, F. Berditshevski, and M.E. Hemler. 2001. Beta1 integrins show specific association with CD98 protein in low density membranes. *BMC Biochem.* 2:10. <http://dx.doi.org/10.1186/1471-2091-2-10>
- Lemaître, G., F. Gonnet, P. Vaigot, X. Gidrol, M.T. Martin, J. Tortajada, and G. Waksman. 2005. CD98, a novel marker of transient amplifying human keratinocytes. *Proteomics.* 5:3637–3645. <http://dx.doi.org/10.1002/pmic.200401224>
- Lemaître, G., A. Stella, J. Feteira, C. Baldeschi, P. Vaigot, M.T. Martin, B. Monsarrat, and G. Waksman. 2011. CD98hc (SLC3A2) is a key regulator of keratinocyte adhesion. *J. Dermatol. Sci.* 61:169–179. <http://dx.doi.org/10.1016/j.jdermsci.2010.12.007>
- Levy, V., C. Lindon, Y. Zheng, B.D. Harfe, and B.A. Morgan. 2007. Epidermal stem cells arise from the hair follicle after wounding. *FASEB J.* 21:1358–1366. <http://dx.doi.org/10.1096/fj.06-6926com>
- Livshits, G., A. Kobiela, and E. Fuchs. 2012. Governing epidermal homeostasis by coupling cell-cell adhesion to integrin and growth factor signaling, proliferation, and apoptosis. *Proc. Natl. Acad. Sci. USA.* 109:4886–4891. <http://dx.doi.org/10.1073/pnas.1202120109>
- Lo, M., Y.Z. Wang, and P.W. Gout. 2008. The x(c)-cystine/glutamate antiporter: a potential target for therapy of cancer and other diseases. *J. Cell. Physiol.* 215:593–602. <http://dx.doi.org/10.1002/jcp.21366>
- Margadant, C., R.A. Charafeddine, and A. Sonnenberg. 2010. Unique and redundant functions of integrins in the epidermis. *FASEB J.* 24:4133–4152. <http://dx.doi.org/10.1096/fj.09-151449>
- Martin, P. 1997. Wound healing—aiming for perfect skin regeneration. *Science.* 276:75–81. <http://dx.doi.org/10.1126/science.276.5309.75>
- Mastroberardino, L., B. Spindler, R. Pfeiffer, P.J. Skelly, J. Loffing, C.B. Shoemaker, and F. Verrey. 1998. Amino-acid transport by heterodimers of 4F2hc/CD98 and members of a permease family. *Nature.* 395:288–291. <http://dx.doi.org/10.1038/26246>
- Mathieu, D., J.-C. Linke, and F. Wattel. 2006. Non-Healing Wounds. In *Handbook on Hyperbaric Medicine*. D. Mathieu, editor. Springer, Netherlands. 401–428.
- Merlin, D., S. Sitaraman, X. Liu, K. Eastburn, J. Sun, T. Kucharzik, B. Lewis, and J.L. Madara. 2001. CD98-mediated links between amino acid transport and beta 1 integrin distribution in polarized columnar epithelia. *J. Biol. Chem.* 276:39282–39289. <http://dx.doi.org/10.1074/jbc.M105077200>
- Meves, A., T. Geiger, S. Zanivan, J. DiGiovanni, M. Mann, and R. Fässler. 2011. Beta1 integrin cytoplasmic tyrosines promote skin tumorigenesis independent of their phosphorylation. *Proc. Natl. Acad. Sci. USA.* 108:15213–15218. <http://dx.doi.org/10.1073/pnas.1105689108>
- Nakamura, E., M. Sato, H. Yang, F. Miyagawa, M. Harasaki, K. Tomita, S. Matsuoka, A. Noma, K. Iwai, and N. Minato. 1999. 4F2 (CD98) heavy chain is associated covalently with an amino acid transporter and controls intracellular trafficking and membrane topology of 4F2 heterodimer. *J. Biol. Chem.* 274:3009–3016. <http://dx.doi.org/10.1074/jbc.274.5.3009>
- Nguyen, H.T., G. Dalmasso, L. Torkvist, J. Halfvarson, Y. Yan, H. Laroui, D. Shmerling, T. Tallone, M. D'Amato, S.V. Sitaraman, and D. Merlin. 2011. CD98 expression modulates intestinal homeostasis, inflammation, and colitis-associated cancer in mice. *J. Clin. Invest.* 121:1733–1747. <http://dx.doi.org/10.1172/JCI44631>
- Nowak, J.A., and E. Fuchs. 2009. Isolation and culture of epithelial stem cells. *Methods Mol. Biol.* 482:215–232. http://dx.doi.org/10.1007/978-1-59745-060-7_14
- Patterson, J.A., M. Eisinger, B.F. Haynes, C.L. Berger, and R.L. Edelson. 1984. Monoclonal antibody 4F2 reactive with basal layer keratinocytes: studies in the normal and a hyperproliferative state. *J. Invest. Dermatol.* 83:210–213. <http://dx.doi.org/10.1111/1523-1747.ep12263581>

- Piwko-Czuchra, A., H. Koegel, H. Meyer, M. Bauer, S. Werner, C. Brakebusch, and R. Fässler. 2009. Beta1 integrin-mediated adhesion signalling is essential for epidermal progenitor cell expansion. *PLoS ONE*. 4:e5488. <http://dx.doi.org/10.1371/journal.pone.0005488>
- Raghavan, S., C. Bauer, G. Mundschau, Q. Li, and E. Fuchs. 2000. Conditional ablation of beta1 integrin in skin. Severe defects in epidermal proliferation, basement membrane formation, and hair follicle invagination. *J. Cell Biol.* 150:1149–1160. <http://dx.doi.org/10.1083/jcb.150.5.1149>
- Ren, X.D., and M.A. Schwartz. 1998. Regulation of inositol lipid kinases by Rho and Rac. *Curr. Opin. Genet. Dev.* 8:63–67. [http://dx.doi.org/10.1016/S0959-437X\(98\)80063-4](http://dx.doi.org/10.1016/S0959-437X(98)80063-4)
- Ren, X.D., W.B. Kiosses, and M.A. Schwartz. 1999. Regulation of the small GTP-binding protein Rho by cell adhesion and the cytoskeleton. *EMBO J.* 18:578–585. <http://dx.doi.org/10.1093/emboj/18.3.578>
- Rintoul, R.C., R.C. Buttery, A.C. Mackinnon, W.S. Wong, D. Mosher, C. Haslett, and T. Sethi. 2002. Cross-linking CD98 promotes integrin-like signaling and anchorage-independent growth. *Mol. Biol. Cell.* 13:2841–2852. <http://dx.doi.org/10.1091/mbc.01-11-0530>
- Rossier, G., C. Meier, C. Bauch, V. Summa, B. Sordat, F. Verrey, and L.C. Kühn. 1999. LAT2, a new basolateral 4F2hc/CD98-associated amino acid transporter of kidney and intestine. *J. Biol. Chem.* 274:34948–34954. <http://dx.doi.org/10.1074/jbc.274.49.34948>
- Rossmann, K.L., C.J. Der, and J. Sondek. 2005. GEF means go: turning on RHO GTPases with guanine nucleotide-exchange factors. *Nat. Rev. Mol. Cell Biol.* 6:167–180. <http://dx.doi.org/10.1038/nrm1587>
- Schäfer, M., and S. Werner. 2007. Transcriptional control of wound repair. *Annu. Rev. Cell Dev. Biol.* 23:69–92. <http://dx.doi.org/10.1146/annurev.cellbio.23.090506.123609>
- Schaller, M.D., J.D. Hildebrand, J.D. Shannon, J.W. Fox, R.R. Vines, and J.T. Parsons. 1994. Autophosphorylation of the focal adhesion kinase, pp125FAK, directs SH2-dependent binding of pp60src. *Mol. Cell. Biol.* 14:1680–1688.
- Schaller, M.D., J.D. Hildebrand, and J.T. Parsons. 1999. Complex formation with focal adhesion kinase: A mechanism to regulate activity and subcellular localization of Src kinases. *Mol. Biol. Cell.* 10:3489–3505.
- Sen, G.L., J.A. Reuter, D.E. Webster, L. Zhu, and P.A. Khavari. 2010. DNMT1 maintains progenitor function in self-renewing somatic tissue. *Nature*. 463:563–567. <http://dx.doi.org/10.1038/nature08683>
- Singer, A.J., and R.A. Clark. 1999. Cutaneous wound healing. *N. Engl. J. Med.* 341:738–746. <http://dx.doi.org/10.1056/NEJM199909023411006>
- Suzuki, N., S. Nakamura, H. Mano, and T. Kozasa. 2003. Galpha 12 activates Rho GTPase through tyrosine-phosphorylated leukemia-associated RhoGEF. *Proc. Natl. Acad. Sci. USA*. 100:733–738. <http://dx.doi.org/10.1073/pnas.0234057100>
- Takesono, A., J. Moger, S. Farooq, E. Cartwright, I.B. Dawid, S.W. Wilson, and T. Kudoh. 2012. Solute carrier family 3 member 2 (Slc3a2) controls yolk syncytial layer (YSL) formation by regulating microtubule networks in the zebrafish embryo. *Proc. Natl. Acad. Sci. USA*. 109:3371–3376. <http://dx.doi.org/10.1073/pnas.1200642109>
- Tscharntke, M., R. Pofahl, A. Chrostek-Grashoff, N. Smyth, C. Niessen, C. Niemann, B. Hartwig, V. Herzog, H.W. Klein, T. Krieg, et al. 2007. Impaired epidermal wound healing in vivo upon inhibition or deletion of Rac1. *J. Cell Sci.* 120:1480–1490. <http://dx.doi.org/10.1242/jcs.03426>
- Tsumura, H., N. Suzuki, H. Saito, M. Kawano, S. Otake, Y. Kozuka, H. Komada, M. Tsurudome, and Y. Ito. 2003. The targeted disruption of the CD98 gene results in embryonic lethality. *Biochem. Biophys. Res. Commun.* 308:847–851. [http://dx.doi.org/10.1016/S0006-291X\(03\)01473-6](http://dx.doi.org/10.1016/S0006-291X(03)01473-6)
- Turchi, L., A.A. Chassot, R. Rezzonico, K. Yeow, A. Loubat, B. Ferrua, G. Lenegre, J.P. Ortonne, and G. Ponzio. 2002. Dynamic characterization of the molecular events during in vitro epidermal wound healing. *J. Invest. Dermatol.* 119:56–63. <http://dx.doi.org/10.1046/j.1523-1747.2002.01805.x>
- Vailly, J., P. Verrando, M.F. Champlaud, D. Gerecke, D.W. Wagman, C. Baudoin, D. Aberdam, R. Burgeson, E. Bauer, and J.P. Ortonne. 1994. The 100-kDa chain of nicein/kalinin is a laminin B2 chain variant. *Eur. J. Biochem.* 219:209–218. <http://dx.doi.org/10.1111/j.1432-1033.1994.tb19932.x>
- Watt, F.M., and H. Fujiwara. 2011. Cell-extracellular matrix interactions in normal and diseased skin. *Cold Spring Harb. Perspect. Biol.* 3:a005124. <http://dx.doi.org/10.1101/cshperspect.a005124>
- White, D.E., N.A. Kurpios, D. Zuo, J.A. Hassell, S. Blaess, U. Mueller, and W.J. Muller. 2004. Targeted disruption of beta1-integrin in a transgenic mouse model of human breast cancer reveals an essential role in mammary tumor induction. *Cancer Cell*. 6:159–170. <http://dx.doi.org/10.1016/j.ccr.2004.06.025>
- Zent, R., C.A. Fenczik, D.A. Calderwood, S. Liu, M. Dellos, and M.H. Ginsberg. 2000. Class- and splice variant-specific association of CD98 with integrin beta cytoplasmic domains. *J. Biol. Chem.* 275:5059–5064. <http://dx.doi.org/10.1074/jbc.275.7.5059>